



Condensing Coatings

**Advanced CARC Coatings for Cleanability and Condensing for
Maintenance and Sustainment**

Final Report

Prepared under:

**NCMS Project No. 140842-B and
Cooperative Agreement HQ0034-15-2-0007
for the**

Commercial Technologies for Maintenance Activities (CTMA) Program

May 2022

**National Center for Manufacturing Sciences
3025 Boardwalk
Ann Arbor, Michigan 48108-3230**

©2022 National Center for Manufacturing Sciences

This Final Report (“Report”) is the property of the National Center for Manufacturing Sciences (NCMS) and is protected under both the U.S. Copyright Act and applicable state trade secret laws. It is delivered under Cooperative Agreement No. HQ0034-15-2-0007 on the express condition that it is not reproduced, in whole or in part, by anyone other than the Department of Defense (DOD) for governmental purposes only.

Neither NCMS, members of NCMS, nor any person acting on behalf of them:

- makes any warranty or representation, express or implied, with respect to the accuracy, completeness or usefulness of the information contained in this Report, or that the use of any information, apparatus, method, or process disclosed in this Report may not infringe privately owned rights; nor
- assumes any liability with respect to the use of, damages resulting from the use of, nor any information, apparatus, method, or process disclosed in this report.

The views and conclusions contained herein are those of the authors and should not be interpreted as necessarily representing the official policies or endorsements, either expressed or implied, of the U.S. Government.

Table of Contents

Section	Page
List of Figures	v
List of Tables	vii
Acronyms and Abbreviations	ix
1. Executive Summary	11
1.1 Results	11
1.2 Benefits	12
1.3 Technology Transition	12
1.4 Invention Disclosure	13
1.5 Project Partners	13
2. Introduction	15
2.1 Background	15
2.2 Purpose	18
2.3 Scope/Approach	18
3. Project Narrative	21
3.1 Coating Development	21
3.1.1 Hydrophobic Silane Cured Coatings	21
3.1.2 Hydrophilic Coatings	22
3.1.3 Electrocoat	23
3.1.4 Miscellaneous Coating Candidates	24
3.2 University of Illinois Screening Tests	25
3.3 National Renewable Energy Lab (NREL) Testing	28
3.3.1 Methodology	30
3.3.2 Heat Exchanger Plenum	30
3.3.3 Fluid Conditioning Facility	33
3.3.4 Sensors	34
3.3.5 Experimental Test Matrix	34
3.3.6 Coated Test Articles	35
3.3.7 Calculations	36
3.3.8 Results	39
4. Conclusions	45
5. Recommendations	47
6. References	49

List of Figures

Figure	Page
1. Wetting States.....	16
2. Images of (a) Filmwise Condensation on Smooth Hydrophilic Copper Tube; (b) Dropwise Condensation on Silane Coated Smooth Copper Tube; (c) Jumping-Droplet Superhydrophobic Condensation on Nanostructured Copper Oxide Tube; (b) Immersion Condensation on Nanostructured Tube with Infused Coating	17
3. Condensation Photos of Wavy Fin and Tube Heat Exchangers With and Without Hydrophilic Coating	17
4. Program Strategy of Coating Development, Lab Scale and Full Heat Exchanger Testing	18
5. WCAs and Hysteresis for Various Fluoropolymer Modified Polysiloxane Coatings.....	21
6. Hardness of Candidate Coating Compositions Along with WCA FOM.....	22
7. Example of High WCA Observed on Candidate Experimental Coatings	22
8. Electrodeposition Coating Process	23
9. Experimental Test Set-Up Testing Coated Copper Tubes for Condensing Efficiency at UIUC	26
10. Close-Up of Coated Tube in Test Apparatus	26
11. Mass Water Collected Relative to WCA.....	27
12. Mass Water Collected Relative to Tilt Angle	27
13. Mass Water Collected Relative to % RH	27
14. Test Matrix Points in Relation to Desired Test Conditions Proposed by GVSC	29
15. TTF Advanced HVAC Laboratory Schematic Depicting Four Inlet and Outlet Air Streams	30
16. Photo of Experimental Apparatus Used to House Heat Exchanger Test Articles.....	30
17. Brazentech 12x12 Finned Coil Air to Water Heat Exchanger	31
18. Illustration of Heat Exchanger Test Stand Showing Key Sensors and Components	31
19. Cross-Sectional View of Heat Exchanger Plenum with Test Article Heat Exchanger, Condensate Drip Pan, Air Battles, and Filters Installed.....	32
20. Heat Exchanger Mounting Fixture and With Heat Exchanger Installed.....	32
21. Heat Exchanger Plenum Access Door and Observation Window	32

22. Glycol Supply and Return Hoses Penetrating into Plenum and Connected to Heat Exchanger	33
23. Heat Exchanger Test Bench Connected to Fluid Conditioning Facility	33
24. Electrocoated Heat Exchanger Fins After Coating and Disassembly	36
25. Uncoated Heat Exchanger; Custom Built 11-Gallon Bath; Top Down View of Bath Filled with Electrodeposition Coating	37
26. Scatter Plot Comparing (a) Moisture Removal Rate and (b) Total Cooling Capacity for Two Uncoated Heat Exchangers	40
27. Scatter Plot Comparing (a) Moisture Removal Rate and (b) Total Cooling Capacity for Two Heat Exchangers with Commercial Radiator Coating	40
28. Average Moisture Removal Rate for All Heat Exchangers Tested at Various Conditions	41
29. Total Cooling Capacity for All Heat Exchangers Tested at Various Conditions.....	41
30. Scatter Plot Comparing (a) Moisture Removal Rate and (b) Total Cooling Capacity for Uncoated and Commercial Radiator Coating Heat Exchangers	41
31. Scatter Plot Comparing (a) Moisture Removal Rate and (b) Total Cooling Capacity for Two Heat Exchangers with Conductive e-Coating	42
32. Scatter Plot Comparing (a) Moisture Removal Rate and (b) Total Cooling Capacity for Commercial Radiator and Conductive Coating Heat Exchangers	42
33. Scatter Plot Comparing (a) Moisture Removal Rate and (b) Total Cooling Capacity for Hydrophobic Coated Heat Exchanger Samples One and Two.....	43
34. Scatter Plot Comparing (a) Moisture Removal Rate and (b) Total Cooling Capacity for Hydrophobic Coated Heat Exchanger Samples Two and Three	43
35. Scatter Plot Comparing (a) Moisture Removal Rate and (b) Total Cooling Capacity for Hydrophilic Coated Heat Exchanger Samples	44
36. Scatter Plot Comparing (a) Moisture Removal Rate and (b) Total Cooling Capacity for Commercial Radiator and Hydrophilic Coated Heat Exchangers.....	44
37. Comparison of Water Collection Rates for Coated Heat Exchangers Relative to Uncoated Control.....	46

List of Tables

Table	Page
1. Standard Planning Factors Related to Personnel in Force (gal/person/day) Conventional Theater	15
2. Water Harvesting Data for Experimental Coatings on Stainless Steel Tubes.....	27
3. Heat Exchanger Coating Configuration for Experiments	29
4. List of Measurements and Sensory Accuracy	34
5. Operation Condition Test Matrix (Sea Level).....	35
6. Operating Condition Test Matrix (TTF Altitude)	36

Acronyms and Abbreviations

Term	Definition	NCMS	National Center for Manufacturing Sciences
CO ₂	Carbon Dioxide		
CTMA	Commercial Technologies for Maintenance Activities	NREL	National Renewable Energy Laboratory
DAQ	Data Acquisition	ODASD-MR	Office of the Deputy Assistant Secretary of Defense, Materiel Readiness
DB	Dry-Bulb		
DOD	Department of Defense	P	Pressure
DP	Dew Point	PDMS	Polydimethyl Siloxane
EES	Engineering Equation Solver	PFPE	Perfluorinated Polyether
EH&S	Environmental Health and Safety	PPG	PPG Industries, Inc.
ETRL	Energy Transport Research Laboratory	RH	Relative Humidity
FOM	Figure of Merit	SCFM	Standard Cubic Feet per Minute
GVSC	Ground Vehicle Systems Center	SOW	Statement of Work
H	Humidity	T	Temperature
HW	Hot Water	TTF	Thermal Test Facility
HVAC	Heating, Ventilating and Air Conditioning	WCA	Water Contact Angle
HX	Heat Exchanger	UIUC	University of Illinois – Urbana Champaign
MFR	Mass Flow Rate	U.S.	United States

1. Executive Summary

Water is critical to life and one of the most important commodities required to sustain military operations. Water is necessary for hydration, food preparation, medical treatment, hygiene, construction, decontamination, maintenance, and many additional tasks. Water support operations consist of treatment, storage, distribution and issue of *potable* and *non-potable water* in a theater of operations. Water supply functions enable freedom of action, extend operational reach, and prolong operational endurance. Depending on the environmental conditions, as much as eight gallons/person/day can be required for drinking, personal hygiene, field feeding, heat injury treatment, and vehicle maintenance. Additional water demands can increase the total daily demand to as much as 16 gallons/person.^[1]

Ensuring continued access to water is necessary for Department of Defense (DOD) installations to achieve their missions however delivering potable water to deployed forces is both dangerous and expensive. One potential way to mitigate the logistical burden of transporting water across long distances is to harvest water from air. The use of a suitable heat exchanger will promote condensation of water on heat exchanger coils which can then be collected for potable and non-potable applications. This project sought to identify coating solutions which could be applied to these coils for improved efficiency and increased volume of water collected. Of particular interest are coatings which promote water collection under low atmospheric humidity conditions.

Funding for a collaborative effort was secured through the National Center for Manufacturing Sciences (NCMS) Commercial Technologies for Maintenance Activities (CTMA) Program and the Office of the Deputy Assistant Secretary of Defense, Materiel Readiness (ODASD-MR).

1.1 Results

A variety of coating formulations were developed and novel test methods developed to assess performance. Typical fin and tube heat exchangers present a challenge to the coatings formulator in that they have a high surface and complex geometries. Conventional spray applied coatings are unable to efficiently reach the interior surfaces of the heat exchanger fins so an immersion process was envisioned that would provide uniform coverage across all surfaces. Further, stable, one-component, aqueous coating compositions would be required to make the process feasible in a manufacturing environment. Fortunately, PPG is a world leader in electrodeposition coatings for a wide range of industrial applications. PPG sought to develop formulations that would provide significant differences in surface energy and/or thermal conductivity in order to test hypotheses about improving heat exchanger efficiency. Formulations were developed that increased hydrophobicity, thermal conductivity or both hydrophobicity and thermal conductivity relative to the electrocoat controls. Further, a unique aqueous immersion coating was developed with hydrophilic properties. The hydrophilic coating was intended as a negative control as the uniform layer of water on condenser surfaces was expected to increase heat transfer resistance.

Testing these various approaches proved much more challenging. Initially the work was supported by researchers at University of Illinois – Urbana Champaign (UIUC). In the UIUC testing 6-inch aluminum tubes were coated with experimental coatings and tested under various conditions of temperature and humidity. Unfortunately, despite excellent collaboration with UIUC, the small tubes provided insufficient surface area for reliable differentiation between the coatings.

Ultimately actual heat exchangers were tested in a custom designed, controlled condition apparatus developed by researchers at the National Renewable Energy Laboratory (NREL). Contrary to initial assumptions, thin film hydrophilic coatings demonstrated an 8% improvement in water harvesting efficiency across a broad range of environmental conditions. The work has applications not only in Army water from air applications but also the commercial heating and ventilation market.

1.2 Benefits

The project has both commercial and military applications. Transporting water to deployed forces in dry regions of the world is both expensive and dangerous. Accordingly, the ability to offset the demand at least partially with water harvested from air could significantly reduce the logistical burden of delivering water. Likewise, commercial heating, ventilating and air-conditioning (HVAC) suppliers are continually looking for ways to improve heat exchanger efficiency and reduce carbon dioxide (CO₂) emissions. In both cases engineered coatings are a potential strategy to improve efficiency of water from air systems.

The commercial heating and cooling market is estimated at over \$100 billion/year with a compound annual growth rate of 5-6%. Currently, coatings are used on heat exchanger surfaces only when HVAC units are deployed in coastal regions where the coatings serve to protect from corrosion. A modest drop in efficiency results from the coatings in this case but is offset by the improved service life. A coating which protects from corrosion and also improves efficiency would therefore be a new to world innovation that could gain significant attention from fabricators of the equipment. In particular, electrodeposition coatings or similar immersion-based application methods would be desirable for this application as they would allow uniform film thickness over the complex fin and tube condenser elements.

In addition to supporting the warfighter and energy savings for commercial customers, coatings which enhance efficiency of air conditioning systems can also support greenhouse gas reductions. Fossil-fuel combustion attributed to residential and commercial buildings accounts for roughly 29% of total U.S. greenhouse gas emissions. Improvements in energy efficiency have led to emission reductions in the residential and commercial sectors of 17.3% and 11.4%, respectively, since a 2005 peak. Major opportunities to reduce emissions from buildings include increased electrification and greater energy efficiency, through the use of “intelligent efficiency” technologies. Capitalizing on those opportunities requires aligning incentives among builders, owners and tenants to favor upfront costs that reduce both emissions and long-term costs.

1.3 Technology Transition

While the research reported here provided surprising insights into heat exchanger coatings which may improve efficiency of water harvesting operations, additional work is required to refine and optimize the approach. Further, once optimized coatings are developed, equipment manufacturers will need to be engaged for integration of the coating with heat exchanger fabrication, a process that may require an additional manufacturing step within the manufacturing facility or the insertion of a toll coater to prepare coated heat exchangers for the equipment manufacturer.

In commercial applications, the same development steps would be required however utilizing a heat exchanger coating in both commercial and military applications would likely enable an overall cost reduction and reduce risks to commercialization. HVAC manufacturers such as Trane are being engaged to assess value of the development in their product portfolio and potentially continue the work using private and/or public funding sources.

1.4 Invention Disclosure

Invention Disclosure Report(s):

DD882 Sent to NCMS ☒

No Inventions (Negative Report) ☐

1.5 Project Partners

- U.S. Army Ground Vehicle Systems Center (GVSC)
- PPG Industries, Inc.
- National Renewable Energy Laboratory (NREL)
- University of Illinois – Urbana Champaign (UIUC)
- National Center for Manufacturing Sciences (NCMS)

2. Introduction

2.1 Background

The DOD document “Water Support Operations, ATP 4-44/MCRP 3-17.7Q, October 2015” provides “information on the doctrinal guidance and direction for U.S. Army and U.S. Marine Corps units conducting water support operations. The techniques provided in this publication are nonprescriptive ways or methods that can be used to perform water support missions, functions, or tasks.” The publication represents a manual for water support operations across both Army and Marine Corps missions. Water support operations include water treatment, storage and distribution and the publication provides insights into the demands and challenges associated with each of these functions. These operations are critical to both Army and Marine Corps deployed forces and they directly impact the depth and duration of military operations.^[1]

The publication provides estimates of water needs assuming a range of environmental conditions and uses. For example, Table 1

details water demands for unit level consumption such as drinking, hygiene and vehicle maintenance but also considers medical treatment, showers and non-potable water needs. As is evident from the table, the demand is high even under favorable environmental conditions. Under hot, arid conditions as our forces are often operating under, the demands can nearly double. Under those conditions the availability of indigenous water sources will be expected to be sparse and the expense and dangers of transporting water will be high.

Access to safe drinking water is not just an issue for our deployed forces, it’s estimated that 2.2 billion people throughout the world are faced with challenges to access of safely managed drinking water.^[2,3] In fact access to safe drinking water is recognized as a global challenge and the United Nations has recognized it as an international development priority by 2030 in the United Nations framework for global development priorities, the Sustainable Development Goals 6.1.^[4]

Table 1. Standard Planning Factors Related to Personnel in Force (gal/person/day) Conventional Theater

Function	Hot				Temperate		Cold	
	Tropical		Arid		Sus	Min	Sus	Min
	Sus	Min	Sus	Min				
Universal Unit Level Consumption ¹	6.91	4.87	7.27	5.23	5.26	3.22	5.81	3.77
Role I and II Medical Treatment	0.03	0.03	0.03	0.03	0.03	0.03	0.03	0.03
Role III and IV Medical Treatment	0.88	0.88	0.88	0.88	0.88	0.88	0.88	0.88
Central Hygiene - Showers	2.07	1.87	2.07	1.87	2.07	1.87	2.07	1.87
Mortuary Affairs Operations	0.03	0.03	0.22	0.22	0.03	0.03	0.03	0.03
Potable Total	9.92	7.68	10.47	8.23	8.27	6.03	8.82	6.58
Centralized Hygiene – Laundry ²	0.26	0.12	0.26	0.12	0.26	0.12	0.26	0.12
Mortuary Affairs Operations	0.19	0.19	NA	NA	0.14	0.14	0.14	0.14
Engineer Construction	1.98	0.00	1.98	0.00	1.98	0.00	1.98	0.00
Aircraft Maintenance	0.14	0.14	0.14	0.14	0.14	0.14	0.14	0.14
Vehicle Maintenance (Non-potable part of UUL)	0.36	0.36	NA	NA	0.19	0.19	0.19	0.19
Non-potable Total³	2.93	0.81	NA	NA	2.72	0.60	2.72	0.60
Theater Total	12.86	8.49	12.86	8.49	10.99	6.63	11.54	7.18
Sus = Sustaining Min = Minimum 1 – Includes gal/person/day requirements for drinking, personal hygiene, field feeding, heat injury treatment, and vehicle maintenance. 2 – Based on a central hygiene goal of two showers and 15 pounds of laundry per Soldier (or Marine) per week. 3 – All potable in arid environment.								

A bewildering array of devices and technologies have been proposed to address this challenge. Many have issues of low yield, particularly in low humidity conditions. Others have not been scaled to provide meaningful impacts to affected communities. Several concepts utilize a wind turbine to generate electrical power which in turn runs a refrigeration unit which collects moisture from the air. While such approaches are elegant in that green energy is used to both create power and produce water, challenges remain with respect to the overall efficiency, scalability and ability to produce water in arid conditions.^[5] Similar systems are in development that utilize photovoltaic energy power condensers to capture water from air.^[6]

Another approach utilizes “fog collectors” to collect water for drinking and irrigation from air. These systems consist of a polypropylene or polyethylene mesh which captures moisture from air and funnels it to collection tanks. They are attractive as they require no external power source but space requirements are high to obtain meaningful volumes of water. As long as the area experiences frequent fog blankets and light wind the approach can be successful even in arid regions.^[7]

In addition to relieving logistical burdens on transporting water across long distances, water harvesting technologies might be employed to improve heat exchanger efficiency in commercial and residential HVAC systems. This would in turn reduce energy demands to obtain comfort levels of temperature and humidity while also reducing greenhouse gas emissions.

Academic researchers have put extensive work into studying heat exchanger efficiency and the role of coatings on heat exchanger surfaces. For example, Ryan Enright et al. provided a review on dropwise condensation which summarized various technical approaches and specifically explored micro and nanostructured surfaces. These authors stated that dropwise condensation is preferred as it provides much higher heat transfer coefficients. However, the required low

surface energy coatings have yet to meet desired cost, durability and performance requirements. Examples include self-assembled monolayers which may be on the order of one nanometer in thickness. In a laboratory environment organo-silanes have been used to achieve very low surface energies and dropwise condensation but durability remains a concern. Polymeric coatings have been proposed to increase durability but coating thickness can increase heat transfer resistance and effectively offset any advantage of dropwise condensation. Plasma enhanced vapor deposition has also been proposed which could deposit a durable, low surface energy coating at very thin film. The problem with this approach becomes cost and scalability.^[8]

Surface roughness modified wetting behavior was also considered and the complexity of different types of condensation that can occur on these surfaces examined. For example, two types of condensation droplets are shown in Figure 1, the Wenzel model of condensation envisions water droplets with high contact angles but wetting of entire surface while the Cassie-Baxter state shows the droplet resting on top of the surface roughness.^[9] The type of droplet formed depends on geometry of surface roughness, nucleation locations and nucleation density. The difference is important as a Wenzel droplet may have excellent adhesion to the surface, increasing thermal conductance but impeding heat transfer, while a Cassie-Baxter droplet is more mobile and favors heat transfer. In practice, a balance would be struck between the two types for optimal performance.^[8]

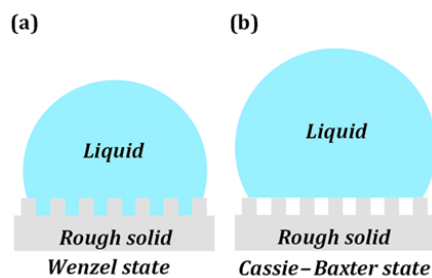


Figure 1. Wetting States

(a) Liquid droplet in Wenzel state;

(b) Liquid droplet in Cassie-Baxter state

Nenad Miljkovic et al. illustrate the various condensation types in a 2013 Journal of Heat Transfer paper.^[10] As shown in Figure 2 film formation, dropwise condensation, jumping droplet and immersion condensation types can be seen. Jumping droplets are created due to the release of excess surface energy which causes the droplet to “jump” from the surface. Immersion condensation occurs where an oil-infused nanostructured surface allows droplets to nucleate immersed in the oil.

Hydrophilic coatings have also been explored by academic researchers. Researchers at the Institute of Refrigeration and Cryogenics in Shanghai, China studied hydrophilic coatings

applied to wavy fin and tube heat exchangers. Of course, condensation on the fin surface occurs when surface temperatures are below the dew point temperature of incoming air. When water condenses as droplets, the individual drops may form bridges between adjacent fins. This in turn reduces heat transfer and increases air pressure drop. Conversely, water on a hydrophilic surface will have a lower contact angle which improves condensate drainage and reduces the pressure drop by as much as 50%. Figure 3 illustrates how the hydrophilic coatings can improve air flow through the condenser elements by preventing the formation of droplets which bridge the fins.^[11]

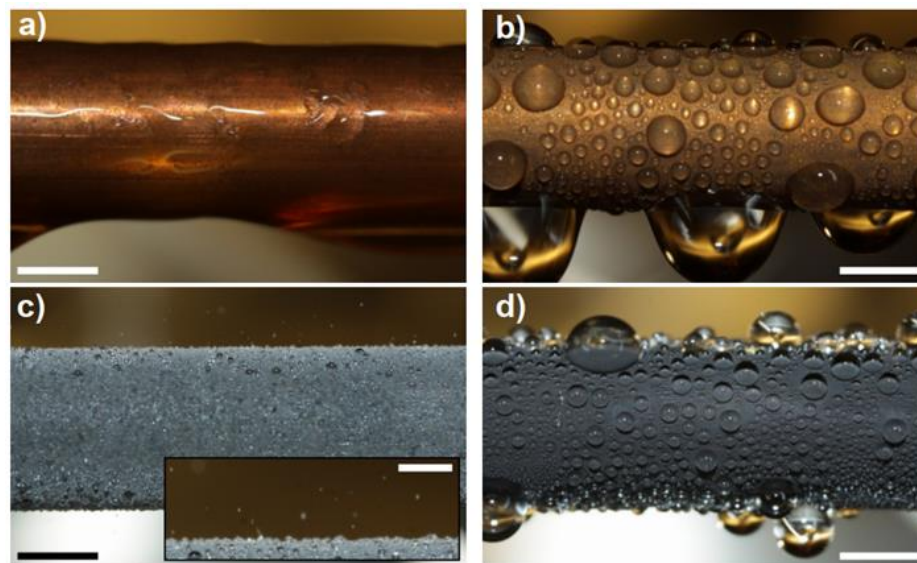


Figure 2. Images of (a) Filmwise Condensation on Smooth Hydrophilic Copper Tube; (b) Dropwise Condensation on Silane Coated Smooth Copper Tube; (c) Jumping-Droplet Superhydrophobic Condensation on Nanostructured Copper Oxide Tube; (d) Immersion Condensation on Nanostructured Tube with Infused Coating

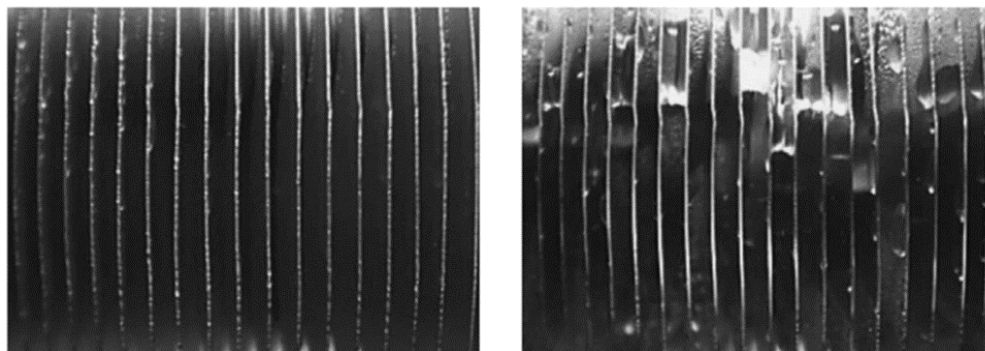


Figure 3. Condensation Photos of Wavy Fin and Tube Heat Exchangers With and Without Hydrophilic Coating ($T_{a,dry} = 27^{\circ}\text{C}$, $RH_{in} = 50\%$, $T_w = 12^{\circ}\text{C}$)

In the Institute of Refrigeration and Cryogenics study heat exchangers with and without a hydrophilic coating were examined. The hydrophilic coating is simply described as an organic resin and the resulting water contact angle (WCA) is between 10 and 20° initially. The authors conclude that the hydrophilic coatings can reduce the air side pressure drops by as much as 44%. However, heat transfer performance is dependent on condensate water state. When bridging between fins can occur, the hydrophilic coating can enhance performance, however under most other conditions the hydrophilic coating weakens heat transfer performance.^[11]

The remainder of this report details the CTMA project's work to develop coatings with a range of surface energy characteristics, apply these coatings to test articles and collect data on rate of condensate collection under various conditions.

2.2 Purpose

The project's purpose was to determine if coatings may be designed which improve efficiency of heat exchangers with a focus on harvesting water from air for deployed forces. While the addition of any coating to heat exchanger surfaces might be expected to reduce efficiency because of increased heat transfer resistance, the team's hypothesis was that efficiency improvements can be achieved by manipulating coating surface energy while maintaining a thin coating to minimize heat transfer resistance. Both hydrophobic and hydrophilic coatings were developed and tested in multiple test configurations and prior to data

collection both approaches could be reasoned to yield the desired improvements. In the case of hydrophobic coatings, the high water contact angle might be expected to facilitate moisture removal from the condenser surfaces. In the case of hydrophilic coatings, the monolayer of water on the condenser surfaces might be expected to reduce bridging of water between fins and reduce the pressure drop from one side of the heat exchanger to the other. The experiments were designed to empirically test these hypotheses and arrive at recommendations for future development work.

2.3 Scope/Approach

The strategy for this work was to first engineer a variety of coatings demonstrating a range of surface energy properties. Initial performance testing was completed using small aluminum tubes as a simplified heat exchanger. Coolant circulated through the tubes and metrics obtained on amount of water collected for a given environmental condition. Based on performance in small scale tests, a subset of coatings were selected for application to actual heat exchangers and tested under more rigorously controlled conditions. Figure 4 illustrates the overall project scheme.

The coatings were designed with several variables in mind. First, to enable uniform coating application over the large surface area and complex geometries, it was desired to have coatings which could be applied via an immersion process. This would ensure complete coverage of the heat exchanger surfaces and allowing the excess material to drain off would

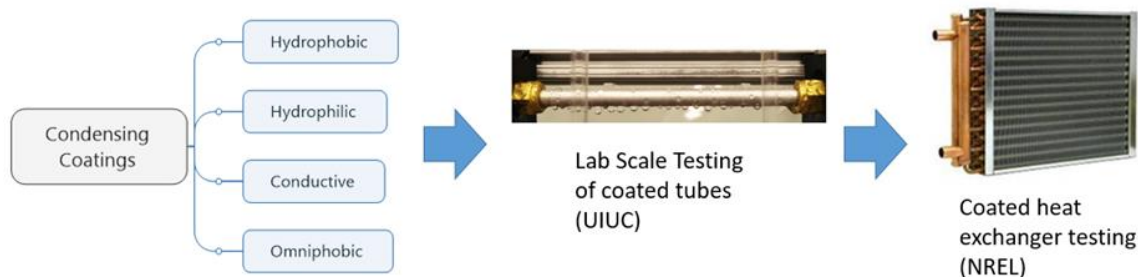


Figure 4. Program Strategy of Coating Development, Lab Scale and Full Heat Exchanger Testing

minimize film thickness differences. Spray applied coatings would not be as desirable since film thickness control throughout the thickness of the heat exchanger would be difficult. Likewise, aqueous coatings were preferred over solvent-based coatings and electrodeposition coatings were determined to be of particular value since some HVAC manufacturers already use electrodeposition primers to protect metal surfaces from corrosion. The team was also cognizant of film thickness throughout development. Leading HVAC manufacturers advised the team that up to about 3 mils the effect on heat transfer resistance can be negligible, however PPG sought to eliminate this variable entirely by keeping coating thickness near 1 mil or less. PPG also chose to use extremes in surface energy to test assumptions and maximize signal to noise ratios in experiments. Hence the coatings were designed to be hydrophobic ($WCA > 100$), hydrophilic ($WCA < 50$) or omniphobic with both hydrophobic and hydrophilic moieties incorporated in the same coating. The team also wanted to examine the role of thermal conductivity by testing some coatings which were marginally electrically conductive with the assumption that electrical conductivity and thermal conductivity often occur in the same types of materials.

Test Plan

Task 1: Develop coatings with a range of surface energy properties as determined by advancing and receding water contact angle measurements.

Task 2: Apply coatings to aluminum tubes for water harvesting experiments at the UIUC campus.

Task 3: Analyze results for guidance on coating optimization.

Task 4: Design experiment and prepare coated articles for larger scale heat exchanger testing at NREL.

Task 5: Analyze results from controlled environment testing at NREL.

Successful completion of Tasks 1-5 would yield design principles and starting point coating formulas for consideration in water harvesting or commercial HVAC applications.

3. Project Narrative

3.1 Coating Development

3.1.1 Hydrophobic Silane Cured Coatings

From a formulation perspective, one- or two-component coatings which are formulated in an organic solvent and applied via spray, dip or draw-down are the easiest way to learn basic design principles which will impart the desired coating properties. However, such an approach is likely to be incompatible with the end application. It will be inefficient and difficult to obtain uniform coating thickness by spraying. Solvent-based immersion coatings would require a bath containing high levels of organic solvents presenting an environmental health and safety (EH&S) barrier and two-component coatings will present a pot-life issue that makes application to heat exchangers in a manufacturing environment impractical. Nonetheless, the approach is an excellent way to discern basic coating design principles which can be applied to electrocoat or water-based immersion coating formulations.

For example, a large sample set was prepared which utilized combinations of silicone and

fluoropolymer resins coupled with various pigment particles. Resulting coatings were spray applied and tested for water contact angle, hysteresis (difference between advancing and receding water contact angle as coated sample is tilted), and tilt angle (angle at which a water droplet begins to roll off the coated surface). Ideally the team believed desired properties for water harvesting applications would be a combination of high WCA coupled with low values for hysteresis or tilt angle. Figure 5 shows that these measures can be obtained but not in all formulations.

The coatings were also tested for overall hardness using a Fischer Microhardness tester. A figure of merit (FOM) was developed based on the average water contact angle minus the hysteresis or tilt angle. Ideally, a candidate coating would have a very high WCA and a very low tilt angle or hysteresis and a high value for Fischer microhardness. As can be seen in Figure 6 the two measures are typically in opposition to each other. Candidate formulations for further exploration would include Formula B which was quite hard and had a moderately high FOM.

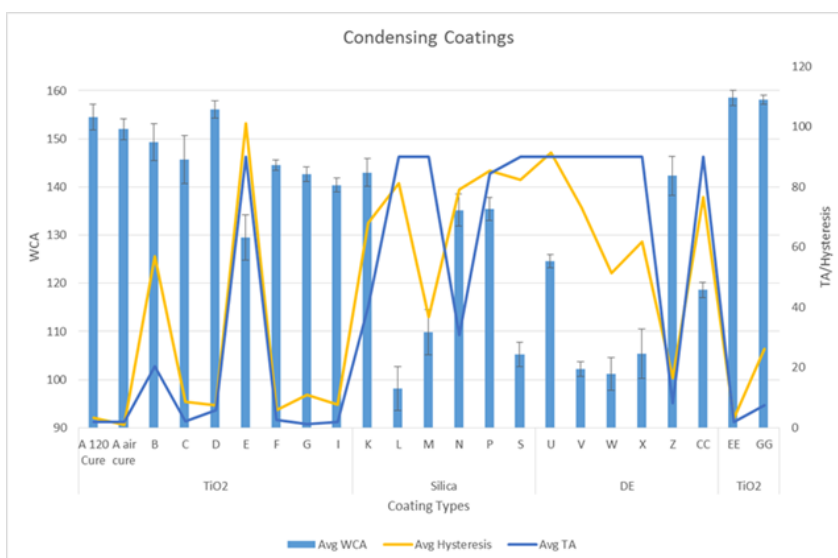


Figure 5. WCAs and Hysteresis for Various Fluoropolymer Modified Polysiloxane Coatings

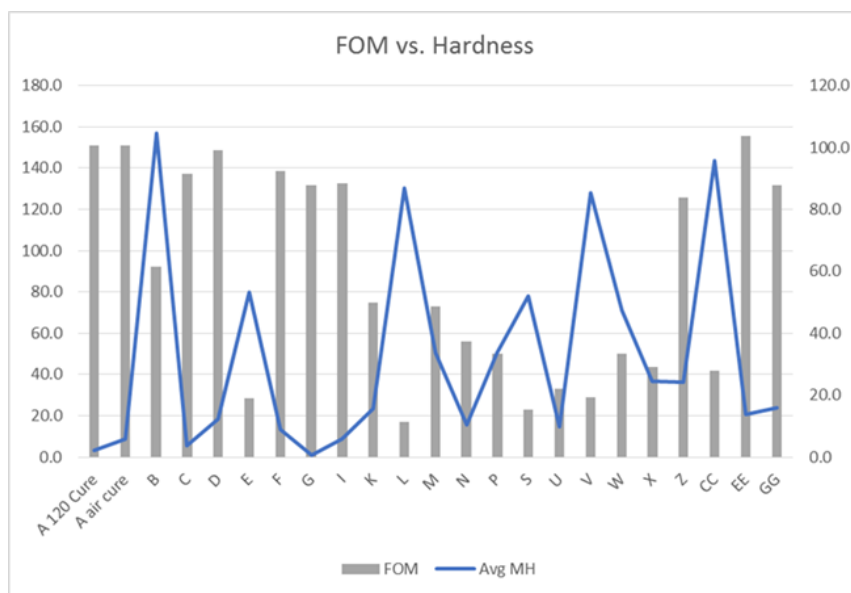


Figure 6. Hardness of Candidate Coating Compositions Along with WCA FOM

Single component coatings with low surface energy were developed by combining silanol terminated polydimethyl and polyfluoropropylmethyl siloxane resins along with alkoxy silane terminated polyurethane resins. The polysiloxane and polyfluoro moieties contribute to low surface energy while the silane terminated polyurethanes provided crosslink density, durability and hardness. From an end use perspective these coatings were not very practical. The resin technology is expensive and coatings were necessarily formulated in organic solvent solutions. However, they provided an excellent combination of high WCA, low sliding angle and hysteresis and were ideal for testing hypotheses about condensation on heat exchanger surfaces (Figure 7).

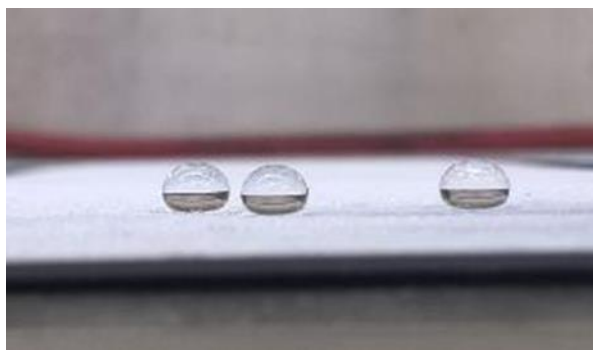


Figure 7. Example of High WCA Observed on Candidate Experimental Coatings

3.1.2 Hydrophilic Coatings

At the other end of the spectrum were hydrophilic coatings. While most literature suggested drop-wise condensation on hydrophobic surfaces would provide the most benefits toward water harvesting, the hydrophilic coatings could serve as a negative control. To produce these formulations PPG synthesized an acrylic polymer with a very high loading of methacryloxy trimethoxy silane (~70%) and some acrylic acid (~5%). The acid was neutralized with dimethyl ethanol amine and the resulting solution dispersed in water. Once dispersed in water the alkoxy silane groups will hydrolyze to silanol groups which in turn partially react to form Si-O-Si linkages upon application. Unreacted Si-OH groups remained in the film and served as the hydrophilic moiety.

Alternative versions on this theme included the addition of a polydimethyl siloxane (PDMS) macromonomer as a portion of the monomer blend. The PDMS backbone provided hydrophobicity while unreacted Si-OH would remain hydrophilic in nature. The macromonomer was also employed in two-component, water dispersible compositions to similarly affect surface energy.

While this coating gave WCA as low as 15° and the benefit of being in water (thus suitable for immersion application techniques), it was not envisioned as a viable commercial solution due to poor durability. Like the hydrophobic coatings mentioned above, these coatings were useful to test theories about heat exchanger performance.

3.1.3 Electrocoat

Electrodeposition coatings are ideal candidates for heat exchanger applications as they are already used by commercial HVAC manufacturers. In particular, HVAC units installed in coastal regions may be electrocoated to protect from corrosion. However, little work has been done to formulate electrodeposition primers for performance properties other than corrosion resistance. Standard, off-the-shelf products will typically have water contact angles of around 75° and high sliding angles so they would be expected to have little utility in water harvesting applications and potentially have a negative impact on heat exchanger efficiency.

The major advantages of the electrocoat process include: total coverage of parts that have complex shapes and interior surfaces with unsurpassed film uniformity; material transfer efficiencies routinely in 95-99% range; highly-automated systems with excellent productivity and low operating costs; fast line speeds and high part racking densities; very low air and wastewater emissions that foster environmental compliance; and a totally enclosed system leading to a cleaner and safer paint application

method. Electrodeposition has demonstrated its value to the automotive industry over the last 40 years. Virtually every car manufactured over this time period has been coated by the electrodeposition process, resulting in improved corrosion performance, reduced environmental emissions, and reduced workplace exposure.

Electrocoat is a process in which electrically charged particles are deposited out of a water suspension to coat a conductive part. During the electrocoat process, high solid material is applied to a part at a controlled film thickness, which is regulated by the amount of voltage applied. The deposition is self-limiting and slows down as the applied coating electrically insulates the part. Electrocoat solids deposit initially in the areas closest to the counter electrode and, as these areas become insulated to current, solids are forced into interior or hidden surfaces to provide complete coverage. This phenomenon is known as throwpower and is a critical aspect of the electrocoat process which also makes it ideal for a complex part such as a heat exchanger.

The electrocoat process can be divided into four distinct sections:

- Pretreatment
- Electrocoat Bath and Ancillary Equipment
- Post Rinses
- Bake Oven

The overall process is illustrated in Figure 8. Parts are first cleaned and pretreated (typically

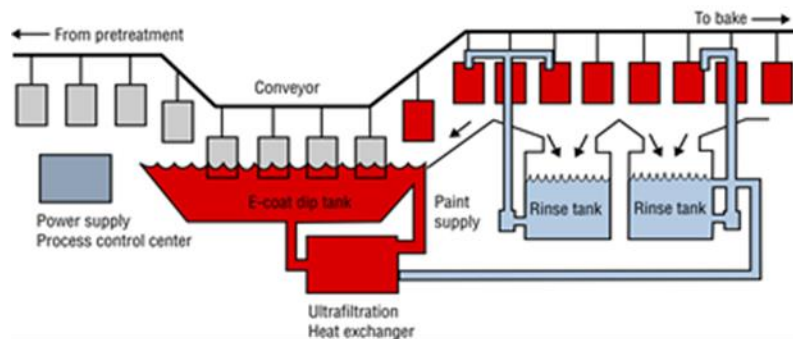


Figure 8. Electrodeposition Coating Process

with a phosphated conversion coating) to prepare the part for electrocoating. Parts are dipped into a coating bath where direct current is applied between the parts and a “counter” electrode. The coating is attracted by the electric field to the part and is deposited on the part. Parts are removed from the bath, rinsed to reclaim undeposited solids, and then baked to cure the deposited material.

Surface energy of electrodeposition coatings was manipulated by the addition of hydrophobic additives such as Fluorolink® E10-H. Fluorolink is a dialcohol terminated, ethoxylated perfluorinated polyether (PFPE). The hydroxyl functional end groups enable covalent bonding and modification of polymers such as urethanes, esters, epoxies and acrylates. Fluorolink E10-H is especially suitable as a building block and polymer modifier for those applications that require a combination of excellent water and oil repellency, easy removal of graffiti and fingerprints, low friction, low refractive index and high chemical resistance. To test the effect of thermal conductivity similar coatings were prepared with carbon black pigments. In addition, coatings were prepared that combined thermal conductivity and low surface energy properties.

3.1.4 Miscellaneous Coating Candidates

Additional coating candidates were selected from commercially available materials and additional PPG developmental approaches. For example, polysilazane resin technology was obtained from EMD Performance Materials. Resins of this type are characterized by a Si-N-Si backbone with organic substituents. Upon hydrolysis they condense to densely crosslinked inorganic networks which have low surface energy and are suitable for high temperature applications. Durazane® 1500 rapid cure organopolysilazane is a low viscosity, methyl substituted organopolysilazane which can be formulated as a one-component coating and cured from room temperature to 250°C. Coatings formulated with Durazane 1500 are

expected to have excellent corrosion protection, easy-clean and high temperature resistance properties.

Another inorganic polymer coating that was examined was a urethane modified sol-gel coating called Gentoo™ from UltraTech International, Inc. Gentoo is a durable hydrophobic multi-functional surface treatment system that has shown exceptional ability to shed water and other fluids such as jet fuel, transmission fluid, and deicing fluid. The coating has led to a significant improvement in both the delay and lower rate of corrosion, including in test cases where Gentoo was applied over-qualified (MIL) paint and plating for the U.S. Military. This reduction in corrosion will directly translate into cost savings through decreased maintenance of certain equipment such as landing gear components and reduced rejection of corroded parts.

The Gentoo treatment exhibits contact angles of $> 110^\circ$ and an average watershed angle of $\sim 3\text{--}11^\circ$, depending on water drop size. Gentoo leaves little to no trail of water, whereas all uncoated substrates leave a significant trail. Gentoo does not affect the transparency of the substrate, exhibiting negligible haze and retention of 100% clarity.^[12] While the water contact and sliding angle data would appear to make this coating ideal for heat exchanger applications, it requires a lengthy mixing and induction time prior to application and has a limited pot-life. As such, use in a continuous manufacturing process as an immersion coating would be difficult to achieve.

Lastly, PPG included novel in-house coatings technology based on aqueous PDMS modified acrylic resin technology. These coatings were formulated as both 1K and 2K compositions with melamine or isocyanate crosslinkers respectively. The melamine crosslinked system in particular could be of value in commercial applications as it could be used in an immersion bath application whereupon cure is only

achieved after the part is removed from the bath and subjected to an elevated bake temperature.

3.2 University of Illinois Screening Tests

Each of the coatings described in this section were used in collaborative experiments with Dr. Nenad Miljkovic of the University of Illinois Energy Transport Research Laboratory (ETRL). Dr. Miljkovic's research intersects the multidisciplinary fields of thermo-fluid sciences, interfacial phenomena, and renewable energy. The lab focuses on efficiency enhancements in energy (power generation, oil and gas, renewables), water, agriculture, transportation and electronics cooling by fundamentally manipulating heat-fluid-surface interactions across multiple length and time scales including fundamental research on micro/nanostructured surfaces for phase change and interfacial phenomena. As such Dr. Miljkovic's lab was an excellent opportunity to collect data on the coatings developed for this project. After a campus visit and survey of the testing and characterization tools available a Statement of Work (SOW) was developed and executed.

Below is a breakdown of the work performed by the Miljkovic lab (ETRL) at UIUC:

Task A – Preparation of tube samples: A full time postdoctoral associate in the Miljkovic lab procured, shaped, installed fittings, and shipped aluminum tube samples to PPG for coating application. Only the outer surfaces were coated for testing. Prior to shipment, tubes were cleaned and installed with Swagelok fittings in order to minimize chance of coating damage. A total of 30 aluminum tubes were shipped, with room for redundancy (multiple tubes per PPG formulation). In addition to shipped tubes, the

UIUC team fabricated control samples (uncoated hydrophilic copper tubes), as well as tubes coated with a superhydrophobic coating enabling “droplet-jumping.”

Task B – Testing of ambient air water harvesting on coated tubes: After receiving the coated tubes from PPG, the Miljkovic lab conducted two separate tests for water collection efficacy. The first test was condensation from ambient air in quiescent (no air flow) conditions. To quantify the water capture efficiency, a custom 3D printed condensate collection tray was used and condensate volume quantified. In order for comparison, a hydraulically balanced header was used to simultaneously test water collection on a control tube with a separate water collection tray. After quiescent conditions were tested, flow conditions were investigated with a low-speed fan (1 m/s). The identical water collection trays were used to quantify water capture. All data collected was analyzed at UIUC and reported to PPG. The experimental set-up and close-up of the coated tube test article can be seen in Figures 9 and 10.

Task C – Testing of water collection on heat exchangers in a wind tunnel: During Task C of the project, the work was intended to be more focused on emulating the real-life water capture conditions encountered by the application end use. To accomplish this heat exchangers with dimensions of 25 cm (length) x 17 cm (width) x 10 cm (depth) were intended to be coated with candidate coatings from the initial studies. However, poor reproducibility of results in the initial phases prevented this task from being performed. The team of PPG and UIUC researchers concluded the small copper tubes had insufficient surface area to make definitive conclusions on coatings to select for this task.

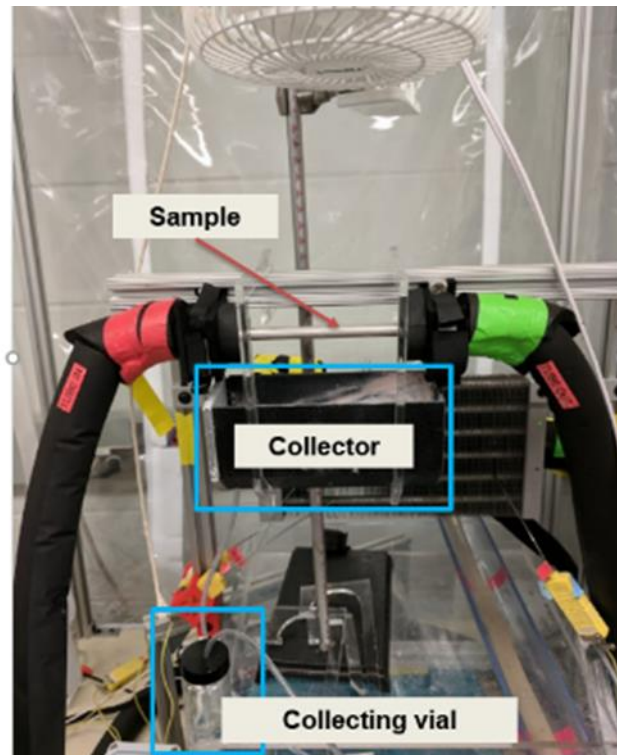
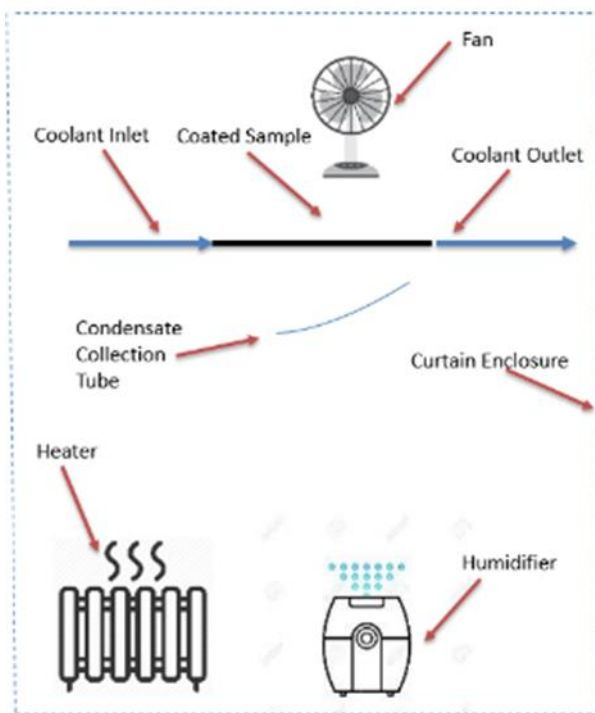


Figure 9. Experimental Test Set-Up Testing Coated Copper Tubes for Condensing Efficiency at UIUC



Figure 10. Close-Up of Coated Tube in Test Apparatus

Once experimental design parameters and equipment were in place PPG coated aluminum tubes with a wide range of coating types with varying values for WCA, hysteresis (the difference between advancing and receding WCA) and tilt angle (the angle of tilt required to initiate the water droplet rolling over the surface). These samples were delivered to UIUC researchers and installed in the test apparatus. Operating conditions were as follows:

- External air flow for assisting removal of collected water from samples

- Air flow of 2 m/s near the tube surface
- Water collected in a closed vial to prevent evaporation
- Total experiment was run for two hours for each sample
- Cooling water was maintained at 0°C
- Ambient temperature and relative humidity (RH) tracked for each sample

The data collected is shown in Table 2. Most of the coated samples provided significantly more water collected than the uncoated control and at

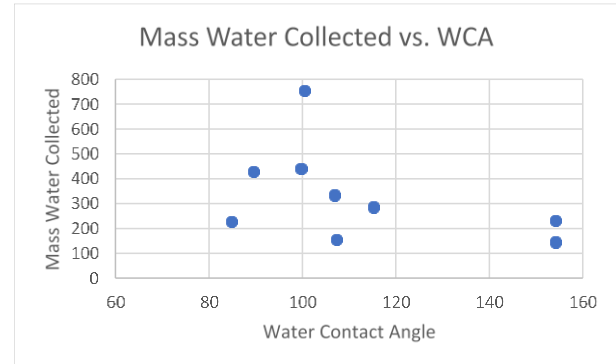
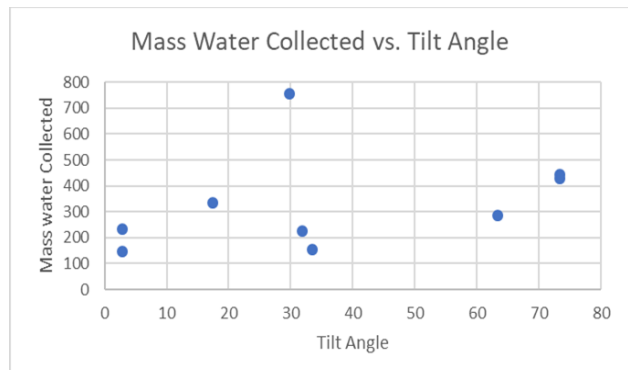
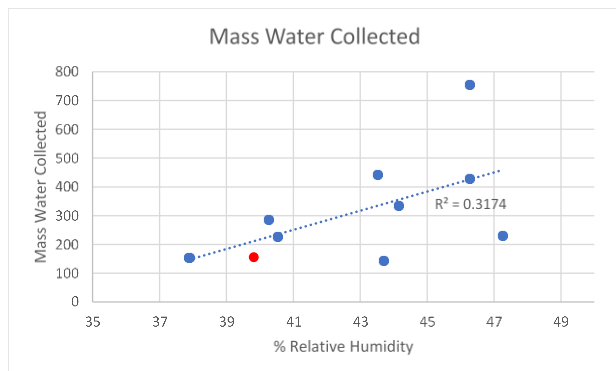
Table 2. Water Harvesting Data for Experimental Coatings on Stainless Steel Tubes

Sample ID	DESCRIPTION	WCA	Hysteresis	Tilt Angle	Cooling water Temperature (°C)	Ambient Temperature (°C)	RH (%)	Mass Water Collected
Control	Uncoated				0	25.78	39.82	155
A	Gentoo™ Urethane modified sol-gel coating	107.3	26	33.4	0	25.92	37.88	155.7
B	Durazane 1500 Rapid Cure Polysilazane coating	84.9	11.7	31.8	0	25.49	40.54	226.7
C	Water based acrylic silanol modified with 15% PDMS macromonomer	89.5	40.7	73.3	0	24.82	46.26	428.3
D	PDMS modified, solvent based 2K urethane	100.5	22.4	29.8	0	29.06	46.26	755.2
E	PDMS modified, solvent based 1K acrylic silane cured coating	154.2	1.8	2.9	0	25.13	47.25	231.4
F	PDMS modified, WB 2K urethane	99.7	28.2	73.4	0	26.83	43.51	442.5
G	PDMS modified, WB 1K acrylic silanol coating	115.2	23.4	63.4	0	25.26	40.25	286.2
H	PDMS-modified, WB 2K melamine crosslinked coating	106.8	19.3	17.5	0	25.23	44.14	335
J	PDMS modified, solvent based 1K urethane silane cured coating	154.2	1.8	2.9	0	24.93	43.7	145

first glance Sample D stands out as having outstanding performance relative to the uncoated control and the other experimental coatings. This is exactly the type of result the project team was hoping to see, however closer examination of the relationship between coating properties and water collected yields a poor correlation. For example, Sample E had nearly ideal properties in terms of water contact angle (154.2°) and tilt angle (2.9°) yet the amount of water collected was modest 231.4 grams. Conversely, Sample D produced a large volume of water (755.2 grams) but had unremarkable measures of WCA (100.5°) and tilt angle (29.8°).

Scatter plots of water mass collected vs. WCA or tilt angle as shown in Figures 11 and 12 illustrate the poor correlation between desired coating properties and water harvesting efficiency. It was expected that increasing WCA and/or decreasing tilt angle would yield higher volumes of water collected, instead the team saw more of a random distribution of the data points.

The mystery was partially solved by plotting mass of water collected vs. % RH as shown in Figure 13 on the following page. While the data is still noisy a general trend is evident where more water was collected at higher RH levels. The red marker in Figure 13 corresponds to the uncoated control tube.

**Figure 11. Mass Water Collected Relative to WCA****Figure 12. Mass Water Collected Relative to Tilt Angle****Figure 13. Mass Water Collected Relative to % RH**

Despite excellent work done by the team at UIUC the data prevented clear conclusions from being drawn with respect to the role of coating surface energy and condensing efficiency. This may have been related to the low surface area the test articles provided. The aluminum tubes were only 4-inches long and ½-inch in diameter. A more realistic and higher surface area solution would be to use fabricated fin and tube heat exchangers and be more representative of real-world applications. Around this time, PPG found a test report on dehumidifier efficiency conducted by Jon Winkler at NREL. The laboratory report documented performance of six residential ENERGY STAR® vapor compression dehumidifiers. A wide range of inlet air conditions were used to assess performance and fit to a numerical model. The R-squared value for both water removal rate and energy factor (i.e. capacity and efficiency) was greater than 0.995 for both. Test data from all six dehumidifiers were fit to a generic performance curve for water removal rate and energy factor. These curves accurately represented all the test data with an average relative error of 5.9% in both estimated water removal rate and estimated energy factor.^[13] Based on the obvious subject matter expertise and specialized equipment the project team engaged with NREL to partner with PPG on the CTMA project. Details on that engagement are detailed in the following section.

3.3 National Renewable Energy Lab (NREL) Testing

Heat exchangers have a wide range of uses in the HVAC industry. One method of improving heat exchanger performance is the application of various coatings to the heat exchanger fin and tube surfaces to increase heat transfer effectiveness, improve moisture removal properties, and mitigate against corrosion. Recently, a series of proprietary coatings were developed by PPG that seek to improve heat exchanger performance. The purpose of this project is to experimentally determine the role of these

proprietary coatings on heat exchanger efficiency and moisture removal rate.

The project performed the three tasks outlined below to determine the impact of the proprietary PPG coatings on heat exchanger performance:

1. Developed Experimental Design – Developed the overall experimental approach, which is described in Section 2 and included the following elements:
 - a. NREL designed experimental apparatus – NREL designed an air plenum capable of providing a wide range of experimental operating conditions and supported quick substitution of heat exchanger test articles. Determined sensor requirements to measure the moisture removal rate of the heat exchangers and calculate air and water mass balances.
 - b. Experimental test matrix – Test matrix was developed in collaboration with NREL and subject matter experts at GVSC. The experimental operating conditions (air dry-bulb temperature, air humidity ratio, and glycol inlet temperature) for each heat exchanger were selected within the bounds of equipment capability at NREL. In most cases NREL was able to meet desired set-points recommended by GVSC but the extreme low humidity conditions were not within system capability. Nonetheless, the selected conditions met much of the design space of interest to the Army and were particularly relevant for commercial HVAC applications (Figure 14).

2. NREL Constructed Experimental Apparatus – NREL acquired the necessary materials and components to construct the experimental apparatus designed in Task 1. Sensors were calibrated and installed and data acquisition program was developed.
3. Collected and Analyzed Experimental Data – NREL measured the performance

of the 12 heat exchangers listed in Table 3 at the operating conditions specified in Task 1. Prior to removing the heat exchanger from the experimental apparatus, the data was analyzed to calculate the heat exchanger moisture removal rate and ensure appropriate mass balances were achieved.

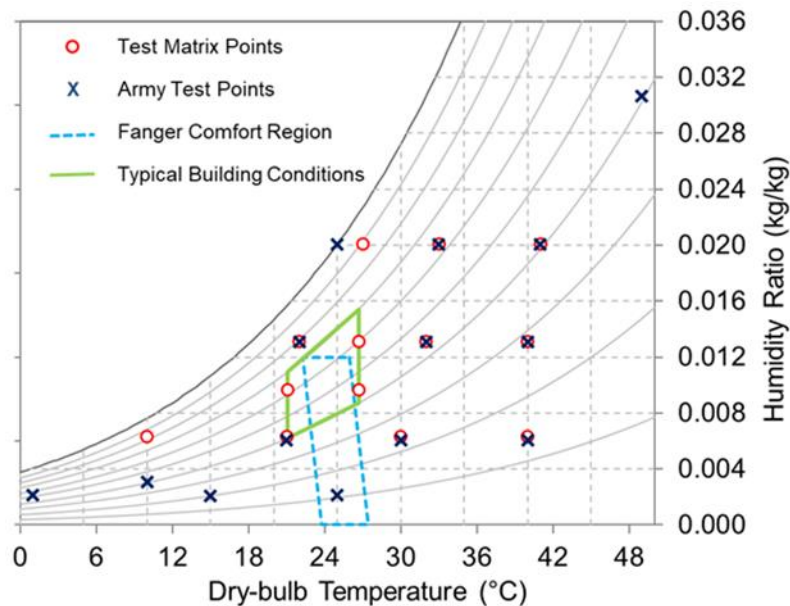


Figure 14. Test Matrix Points in Relation to Desired Test Conditions Proposed by GVSC

Table 3. Heat Exchanger Coating Configuration for Experiments

Heat Exchanger ID	Coating Type
1	Uncoated (control)
2	
3	Cationic epoxy electrodeposition coating (commercial radiator coating)
4	
5	Cationic acrylic electrodeposition coating modified with Fluorolink® E10-H (dialcohol terminated, ethoxylated PFPE for hydrophobicity)
6	
7	Cationic acrylic electrodeposition coating modified with carbon black to increase conductivity
8	
9	
10	Aqueous dispersion of acrylic silanol resin
11	
12	Aqueous dispersion of acrylic silanol resin (repeat with fresh resin sample)

The heat exchangers listed in Table 3 differs from the original set of heat exchangers listed in the project's SOW. It should be noted that heat exchanger #9 was added due to variability in performance of heat exchangers #7 and #8. Heat exchanger #12 was added to further investigate the performance of the hydrophilic coating since the performance of heat exchangers #10 and #11 exceeded expectations.

3.3.1 Methodology

The experimental portion of this study was performed using the Advanced HVAC Laboratory located in NREL's Thermal Test Facility (TTF) in Golden, CO. The TTF is an 11,000 sq.-ft. multi-purpose laboratory facility that enables detailed evaluation and development of building and thermal energy systems.

The Advanced HVAC Laboratory is a 100% outdoor air psychrometric laboratory that delivers conditioned air to the heat exchanger using a custom, computer-based measurement and data acquisition system to control and maintain precise air temperature, humidity, pressure, and flow rate. Two laboratory (one supply and one exhaust) air streams were used to control and measure the psychrometric conditions at the inlet and outlet of the heat exchanger. Accurate, real-time measurements were recorded to determine the heat transfer performance of the heat exchanger. Figure 15 highlights the HVAC laboratory layout of four inlet and exhaust airstreams, two of which were used to measure the heat exchanger performance.

A custom-built heat exchanger plenum was developed to interface with the Advanced HVAC Laboratory and house the test article heat exchangers, which is shown in Figure 16.

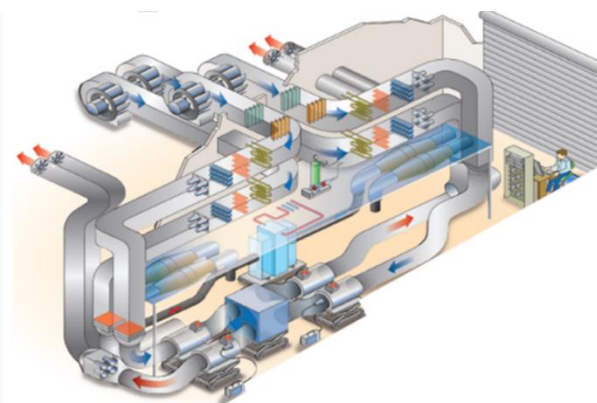


Figure 15. TTF Advanced HVAC Laboratory Schematic Depicting Four Inlet and Outlet Air Streams

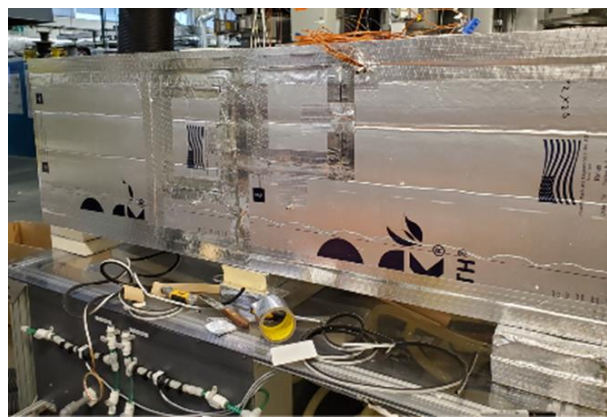


Figure 16. Photo of Experimental Apparatus Used to House Heat Exchanger Test Articles

3.3.2 Heat Exchanger Plenum

The heat exchanger test stand was developed to hold the test articles in place during the experiments, while directing well-mixed conditioned air through the heat exchanger and collecting the condensate. The heat exchanger test stand was designed to quickly remove and install test article heat exchangers, while also allowing for a broad range of data acquisition (DAQ) sensors to be installed near the heat exchanger. The test articles were purchased from Brazentech Heat Exchangers and were selected based on the need to have a large surface area of fins for coating while having an overall size suitable for immersion in a small electrodeposition bath. The item selected had approximate dimensions of 12" x 12" x 3" as shown in Figure 17.



Figure 17. Brazentech 12x12 Finned Coil Air to Water Heat Exchanger

Figure 18 shows a schematic of the heat exchanger air plenum depicting the heat exchanger location, the sensors installed to measure performance, as well as the airflow path and mixing elements. Air flows from left to right in the schematic. A series of baffles and filters were installed at the plenum inlet and outlet to assist with mixing and to achieve a uniform distribution of air at the heat exchanger air inlet and prior to the outlet-side measurements. The DAQ instrumentation installed in the heat exchanger plenum included dry-bulb temperature (T), dew-point temperature (humidity [H]), and static pressure (P) measurements. Condensate was collected in a drip pan and flowed through a Coriolis meter to measure the moisture removal rate.

The heat exchanger test stand was constructed using expanded polystyrene foam panels to minimize thermal gains/losses and sealed using HVAC-grade aluminum foil tape to prevent air leakage.

Figure 19 shows a cross-sectional view of the heat exchanger air plenum taken prior to attaching the inlet/outlet air streams hoses used to connect the plenum to the laboratory-controlled air streams. A heat exchanger mounting frame was assembled and placed in the plenum to ensure the heat exchanger was secured perpendicular to the air flow and oriented in a vertical position to facilitate dripping of condensation into the drip pan. Figure 20 shows an image of the heat exchanger mounting frame with and without the heat exchanger installed.

Additionally, an access door with a plexiglass observation window were added to a side panel of the plenum in order to easily access, remove, and insert heat exchangers and to help monitor the experiments for condensation (Figure 21).

Finally, two cut-outs were placed on the side panel of the plenum opposite from the access door to route the glycol supply and return hoses. The image in Figure 22 shows the cold glycol supply and return hoses being routed into the plenum and connected to the heat exchanger under test.

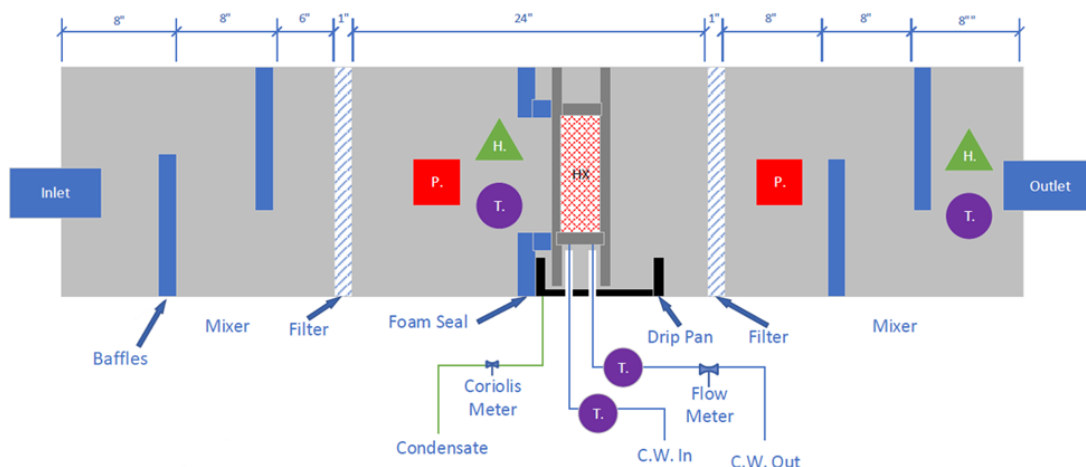


Figure 18. Illustration of Heat Exchanger Test Stand Showing Key Sensors and Components

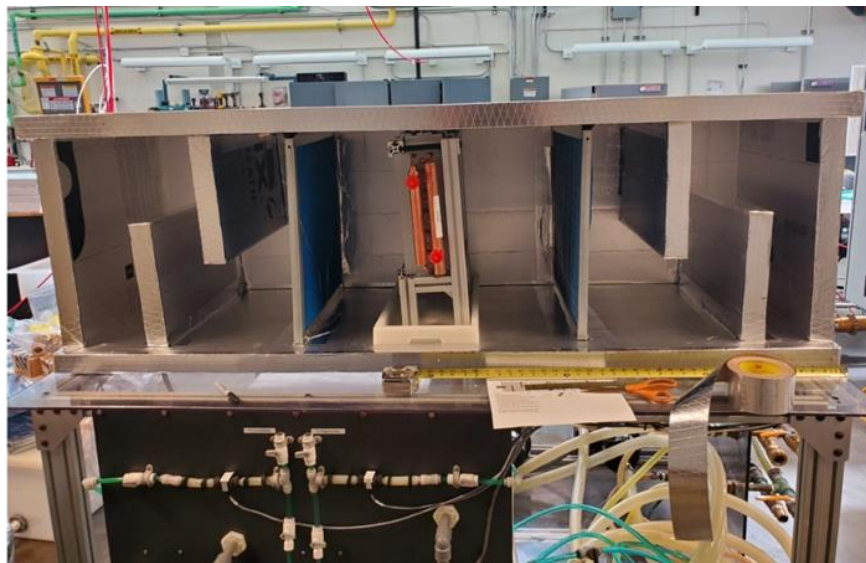


Figure 19. Cross-Sectional View of Heat Exchanger Plenum with Test Article Heat Exchanger, Condensate Drip Pan, Air Baffles, and Filters Installed

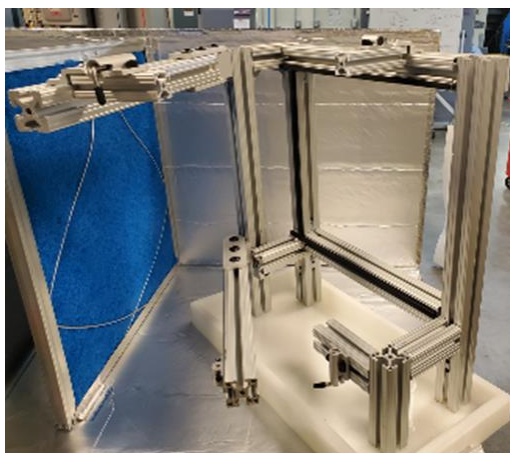


Figure 20. Heat Exchanger Mounting Fixture (left) and With Heat Exchanger installed (right)

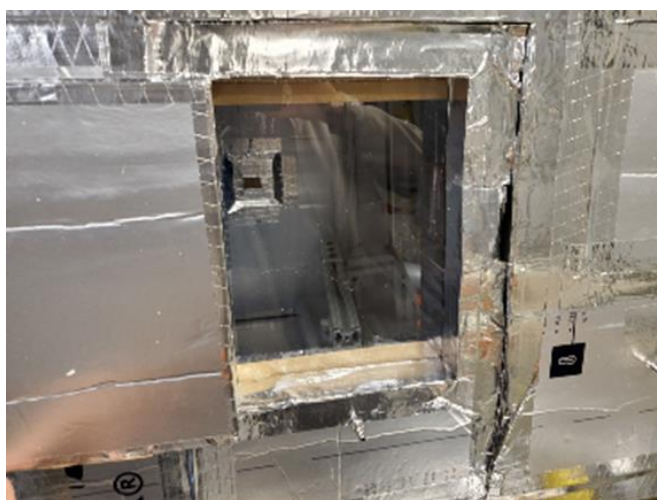


Figure 21. Heat Exchanger Plenum Access Door (left) and Observation Window (right)



Figure 22. Glycol Supply and Return Hoses Penetrating into Plenum and Connected to Heat Exchanger

3.3.3 Fluid Conditioning Facility

Cold glycol was supplied to the heat exchanger using a secondary loop thermally connected with a 20-ton (70.2 kW) capacity chiller loop, which conditioned the glycol to the desired temperature. As previously mentioned, the heat exchanger plenum was connected to the inlet/outlet air streams of the HVAC laboratory. The glycol-side of the heat exchanger was connected to a fluid conditioning facility to provide a precisely controlled inlet glycol temperature. Figure 23 shows a full schematic of the heat exchanger plenum connected to the fluid conditioning facility, as well as several temperature, pressure, and humidity measurements described in previous section. Note that the hot-water (HW) loop drawn in Figure 23 with gray lines was not used in these experiments.

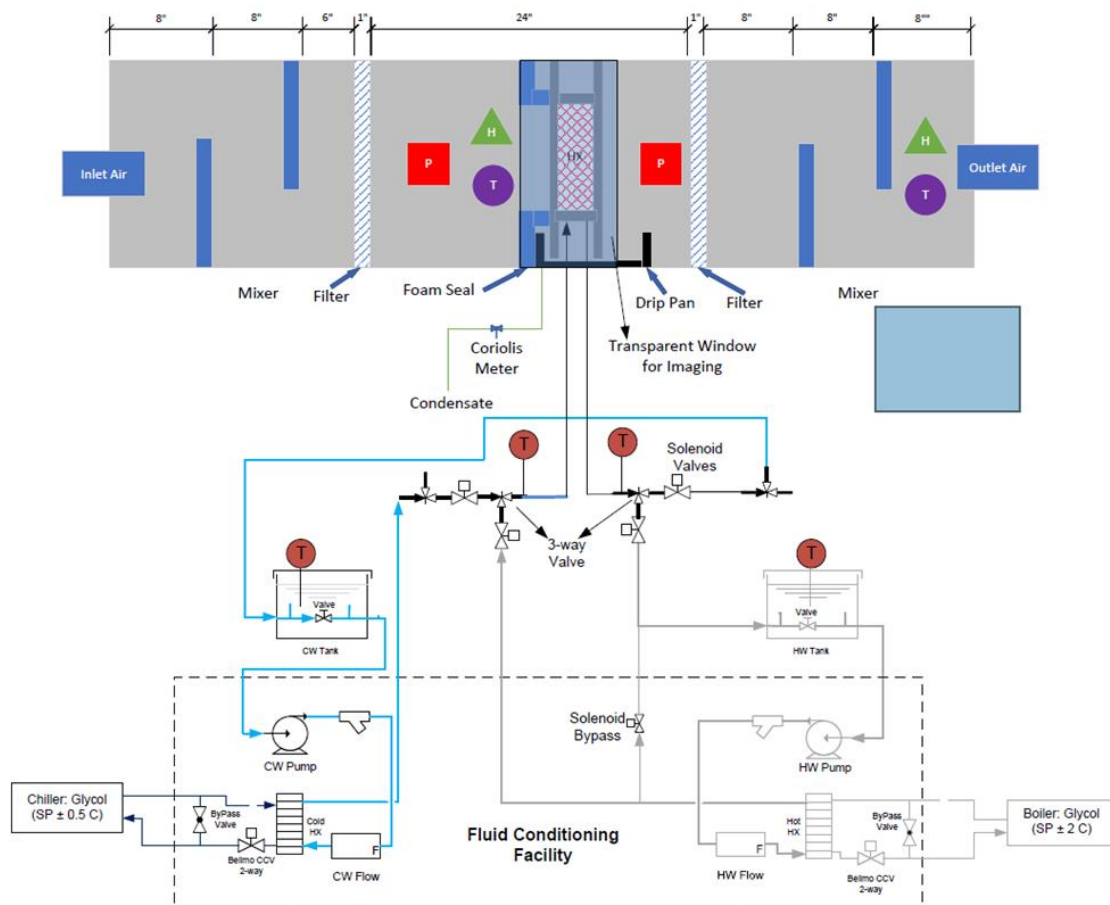


Figure 23. Heat Exchanger Test Bench Connected to Fluid Conditioning Facility

3.3.4 Sensors

The following measurements were collected and used to analyze heat exchanger performance:

1. Air-side inlet and outlet dry-bulb (DB) temperature, dew point (DP) temperature, static pressure, and mass flow rate (MFR).
2. Glycol-side inlet and outlet temperature and volumetric flow rate.
3. Condensate MFR.

Table 4 lists the sensors and devices used to gather key measurements, the location/description of these sensors, and the manufacture-specified accuracy.

3.3.5 Experimental Test Matrix

A test matrix was developed to ensure a wide and complete range of operating conditions to quantify the impact of the heat exchanger coatings. Table 5 lists the operating condition test matrix for sea level barometric pressure with operating conditions grouped by the dew

point temperature. Test Point 1b was added to provide additional granularity between Test Points 1 and 2 and Test Point 9b was added after shakedown testing since Test Point 9 had low moisture removal rates. Test Point 4 was eventually removed from the experiments since the heat exchangers did not remove a detectable amount of moisture from the air stream.

The air mass flow rate and glycol volumetric flow rate were determined using specifications provided by the heat exchanger manufacturer and held constant for all operating conditions. The air mass flow rate was 350 standard cubic feet per minute (SCFM) and the glycol volumetric flow rate was 22.7 L/min.

It is important to note that the operating conditions shown in Table 5 are those corresponding to sea-level conditions. Since the TTF is in Golden, CO, which is located at an elevation of 5,827 ft. above sea level, a series of calculations were conducted to adjust for the barometric pressure present at this higher elevation.

Table 4. List of Measurements and Sensory Accuracy

Location	Measurement	Sensor Description	Accuracy
Air-side	Inlet air DB temperature	T-type thermocouple array	$\pm 0.50^{\circ}\text{C}$
	Inlet air DP temperature	General Eastern SIM-12H DP hygrometer	$\pm 0.25^{\circ}\text{C}$
	Inlet air mass flow rate	Meriam model #50MC2 laminar flow element	$\pm 0.86\%$
	Outlet air DB temperature	T-type thermocouple array	$\pm 0.50^{\circ}\text{C}$
	Outlet air DP temperature	General Eastern SIM-12H DP hygrometer	$\pm 0.25^{\circ}\text{C}$
	Outlet air mass flow rate	Meriam model #50MC2 laminar flow element	$\sim \pm 2.0\%^1$
	Diff. pressure (outlet-inlet)	Setra Model #239	$\pm 0.14\% \text{ FS}$
	Diff. pressure (outlet-ambient)	Setra Model #239	$\pm 0.14\% \text{ FS}$
Glycol-side	CW Tank Temperature	Inline T-type thermocouple	$\pm 0.50^{\circ}\text{C}$
	Inlet temperature	Inline T-type thermocouple	$\pm 0.50^{\circ}\text{C}$
	Outlet temperature	Inline T-type thermocouple	$\pm 0.50^{\circ}\text{C}$
	Diff. pressure (inlet-outlet)	Setra Model #239	$\pm 0.14\% \text{ FS}$
	Glycol volumetric flow rate	Omega model #FTB605	$\pm 1.5\%$
HX test bench	Condensate mass flow rate	Micro Motion Coriolis meter	$\pm 0.5\%$
Facility	Barometric pressure	MKS Baratron 220D	$\pm 0.15\%$

* Determined through uncertainty propagation analysis accounting for facility nozzle pressure transducer and thermocouple accuracy, and uncertainty in the nozzle discharge coefficients.

Table 5. Operation Condition Test Matrix (Sea Level)

Test Point	DB Temperature		DP Temperature		Humidity Ratio		Relative Humidity	Glycol Inlet Temperature
	(°C)	(°F)	(°C)	(°F)	(g/kg)	(grains)	(%)	(°C)
1	10.0	50.0					82.8	
1b	15.5	50.0					57.8	
2	21.0	69.8	7.2	45.0	6.31	44.2	40.9	-0.3
3	30.0	86.0					24.0	
4	40.0	104.0					13.8	
5	21.1	70.0					61.8	
6	26.7	80.0	13.5	56.3	9.65	67.5	44.2	5.9
7	22.0	71.6					79.0	
8	26.7	80.0					59.7	10.7
9	32.0	89.6	18.2	64.8	13.11	91.8	43.9	
9b	32.0	89.6					43.9	
10	40.0	104.0					28.3	7.7
11	27.0	80.6					88.8	
12	33.0	91.4	25.0	77.0	20.09	140.6	63.0	17.4
13	41.0	105.8					40.7	

Yin and Sang (2020) developed a simulation-based procedure to correct for barometric pressure variation when testing hydronic cooling coils that results in sea-level equivalent sensible and latent capacity.^[14] The first step was to simulate the uncoated heat exchanger to estimate the heat exchanger performance at sea level using a previously developed and validated glycol-to-air heat exchanger model written using Engineering Equation Solver (EES). The coil bypass factor was determined using the operating conditions listed in Table 5. The approach developed by Yin and Sang uses the coil bypass factor to adjust the entering wet-bulb temperature to maintain a constant enthalpy difference between the entering moist air and wet heat exchanger surface.

The operating condition test matrix listed Table 5 was adjusted using the EES model and the procedure developed by Yin and Sang (2020), and the altitude-adjusted test matrix is listed in Table 6. Note that procedure by Yin and Sang adjusts only the coil inlet humidity, thus the air dry-bulb and glycol inlet temperatures are the same in Table 5 and Table 6. The adjustment procedure results in slightly lower

inlet air dew point temperatures to maintain sea level equivalent operating conditions.

3.3.6 Coated Test Articles

The coatings as described in Table 3 were developed by PPG and tested on aluminum coupons before attempting to coat heat exchangers for the NREL testing. The hydrophilic coating was comprised of an acrylic resin with pendant alkoxy silane groups. Once neutralized and inverted in water these silanol groups hydrolyzed to silanol groups which provided hydrophilicity as well as a means to introduce crosslinking once the coating was applied and allowed to cure at ambient temperatures. The formulation was applied to heat exchangers as a low solids, one-component aqueous solution by immersing the heat exchanger in a bath of the coating and allowing excess material to drain away. The resulting film measured about 0.3 mils in total thickness. While the low film thickness was expected to have minimal effect on heat transfer resistance, long-term durability was expected to be an issue to examine in subsequent experiments.

Table 6. Operating Condition Test Matrix (TTF Altitude)

Test Point	DB Temperature		DP Temperature		Humidity Ratio		Relative Humidity (%)	Glycol Inlet Temperature (°C)
	(°C)	(°F)	(°C)	(°F)	(g/kg)	(grains)		
1	10.0	50.0					80.1	
1b	15.5	50.0					55.8	
2	21.0	69.8	6.7	44.1	7.57	53.0	39.5	-0.3
3	30.0	86.0					23.2	
4	40.0	104.0					13.3	
5	21.1	70.0	12.9	55.3	11.56	80.9	59.6	5.9
6	26.7	80.0					42.6	
7	22.0	71.6					76.4	
8	26.7	80.0					57.7	10.7
9	32.0	89.6	17.7	63.8	15.76	110.4	42.5	
9b	32.0	89.6					42.5	
10	40.0	104.0					27.4	7.7
11	27.0	80.6					85.9	
12	33.0	91.4	24.4	76.0	24.23	169.6	60.9	17.4
13	41.0	105.8					39.4	

In contrast, the electrodeposition coatings were more difficult to coat as the bath would need to accommodate the part, cathode, heaters and mechanical stirrers. As the Brazentech heat exchangers were too large for the lab scale electrodeposition baths, a custom-designed container was built to accommodate immersing an entire heat exchanger. This required a total paint volume of 11 gallons for each formula variation. Likewise process variables had to be optimized to ensure complete and uniform coating thickness throughout the entire depth of the heat exchangers. This was accomplished by sawing the 12-inch square heat exchangers into four smaller sections which could be coated in lab-scale electrocoat baths. These sections were then disassembled to observe and measure film thickness throughout the depth of fins. Evidence of complete coverage is seen in Figure 24 which shows complete coverage on the individual fin elements after coating and disassembly.

Once process variables were optimized the full-size heat exchangers could be coated in the larger bath. Figure 25 shows the test article heat exchanger, 11-gallon bath, pumps and cathode elements. The various electrodeposition

formulas were applied to three heat exchangers each with the best two samples being sent to NREL for testing. After each formulation was used, the bath was emptied, cleaned and refilled with the next formulation under investigation until samples had been prepared with all formula modifications.

3.3.7 Calculations

The primary performance metrics used to evaluate the heat exchanger performance were moisture removal rate ($\dot{m}_{moisture}$), which is equivalent to the latent heat transfer (\dot{Q}_{lat}), and the total heat transfer rate (\dot{Q}_{total}). The moisture



Figure 24. Electrocoated Heat Exchanger Fins After Coating and Disassembly



Figure 25. Uncoated Heat Exchanger (left); Custom Built 11-Gallon Bath (center): Top Down View of Bath Filled with Electrodeposition Coating (right)

removal rate and rate of total heat transfer were determined for each operating condition and compared for each heat exchanger sample.

The heat exchanger moisture removal rate ($\dot{m}_{moisture}$) was determined by taking the mean of air moisture removal rate ($\dot{m}_{air,moisture}$) and the condensate mass flow rate (\dot{m}_{cond}).

$$\dot{m}_{moisture} = 0.5 \cdot (\dot{m}_{air,moisture} + \dot{m}_{cond}) \quad (1)$$

The air moisture removal rate was calculated using the difference between the inlet humidity ratio (ω_{in}) and the outlet humidity ratio (ω_{out}) as shown in Equation 2.

$$\dot{m}_{air,moisture} = \dot{m}_{air}(\omega_{in} - \omega_{out}) \quad (2)$$

The condensate moisture removal rate (\dot{m}_{cond}) was determined by placing the outlet of the Coriolis meter into a small bucket and then measuring the mass of condensate collected during a 30-minute test period. It is important to note that the 30-minute test period was initiated after steady state conditions were achieved. Measuring the mass of the condensate was done to avoid fluctuations in the Coriolis meter output and to ensure an accurate measurement. It should be noted that the output of the Coriolis meter was also registered and used to compare with the total mass measurement.

The latent heat transfer rate (\dot{Q}_{lat}) was calculated using Equation 3.

$$\dot{Q}_{lat} = \dot{Q}_{total} - \dot{Q}_{sens} \quad (3)$$

where the total heat transfer rate (\dot{Q}_{total}) was the mean of the air total heat transfer rate ($\dot{Q}_{air,total}$) and the glycol heat transfer rate (\dot{Q}_{glycol}).

$$\dot{Q}_{total} = 0.5 \cdot (\dot{Q}_{air,total} + \dot{Q}_{glycol}) \quad (4)$$

where

$$\dot{Q}_{air,total} = \dot{m}_{air}(h_{air,in} - h_{air,out}) - \dot{m}_{air,moisture}C_{p,w}W_{out} \quad (5)$$

and

$$\dot{Q}_{glycol} = \dot{m}_{glycol}C_{p,g}(T_{cg,in} - T_{cg,out}) \quad (6)$$

The air-side total heat transfer rate (Equation 5) was calculated using the air mass flowrate (\dot{m}_{air}), the inlet air enthalpy ($h_{air,in}$), the outlet air enthalpy ($h_{air,out}$), the moisture removal rate ($\dot{m}_{air,moisture}$), specific heat of water ($C_{p,w}$), and the outlet air wet-bulb temperature (W_{out}). The glycol heat transfer rate (Equation 6) was calculated using the mass flowrate of glycol (\dot{m}_{glycol}), the specific heat of glycol flowing through the heat exchanger ($C_{p,g}$), and the chilled glycol inlet and outlet temperatures ($T_{cg,in}$, $T_{cg,out}$).

The sensible heat transfer rates in Equation 3 (\dot{Q}_{sens}) was calculated using Equation 7.

$$\dot{Q}_{sens} = \dot{Q}_{air,sens} \left(\frac{\dot{Q}_{total}}{\dot{Q}_{air,total}} \right) \quad (7)$$

where

$$\dot{Q}_{air,sens} = \dot{m}_{air} C_{p,air} (T_{air,in} - T_{air,out}) \quad (8)$$

where $T_{air,in}$ and $T_{air,out}$ represent the average dry-bulb temperature measured at the heat exchanger inlet and outlet, respectively, and $C_{p,air}$ is the specific heat of air.

Equations 1-8 are based on ASHRAE Standard 33 – Methods of Testing Forced-Circulation Air-Cooling and Air Heating Coils (ASHRAE 2016).^[15]

Lastly, mass and energy balance calculations were performed to ensure proper operation of the heat exchanger test bench and accurate measurements of the heat exchanger performance metrics. The mass balance is performed for the air mass flow rate (ε_{mass}), water mass flow rate (ε_{water}), and energy transfer (ε_{energy}). The balance equations are shown in Equations 9-11.

$$\varepsilon_{mass} = \frac{\dot{m}_{air,in} - \dot{m}_{air,out}}{0.5(\dot{m}_{air,in} + \dot{m}_{air,out})} \quad (9)$$

$$\varepsilon_{water} = \frac{\dot{m}_{air,moisture} - \dot{m}_{cond}}{\dot{m}_{moisture}} \quad (10)$$

$$\varepsilon_{energy} = \frac{\dot{Q}_{air,total} - \dot{Q}_{glycol}}{\dot{Q}_{total}} \quad (11)$$

For the mass and energy balances shown in Equation 9-11, the criteria to ensure proper operation of the heat exchanger test bench, steady-state operating conditions, and accurate measurements of the heat exchanger performance metrics is an absolute value of less than 5%. Equations 12-14 outline the 5% deviation criteria used for the respective balance type.

$$|\varepsilon_{mass}| \leq 5\% \quad (12)$$

$$|\varepsilon_{water}| \leq 5\% \quad (13)$$

$$|\varepsilon_{energy}| \leq 5\% \quad (14)$$

3.3.8 Results

The following section discusses key results observed during this study. It is important to note that the primary metrics of interest for the heat exchanger coatings are the moisture removal rate ($\dot{m}_{moisture}$) and the total cooling capacity (\dot{Q}_{total}). As mentioned previously, the output of the Coriolis meter, which was used to measure moisture removal, tends to fluctuate due to the nature of the meter. Therefore, in addition to recording the Coriolis output, the total mass of condensate removed was collected and measured over a 30-minute period to get a second reading of condensate removal rate (\dot{m}_{cond}).

Two heat exchangers for each coating type were tested to assess variability in heat exchanger performance and consistency with the coating process. Figure 26 compares the moisture removal rate and total cooling capacity for the two uncoated heat exchangers. The solid line equals perfect agreement between the two heat exchangers and the dashed lines represent $\pm 5\%$ variation. Figure 26 shows there is little variation between the two uncoated heat exchangers and the experimental apparatus achieved consistent results for comparing heat exchanger performance.

Figure 27 includes similar plots for the two heat exchangers with the commercial radiator coating. There was slightly more variation in the measured moisture removal rate for the two heat exchangers with the commercial radiator coating.

Figure 28 shows the moisture removal rate for all the heat exchangers tested determined by the condensate mass measurement and Figure 29

shows the total cooling capacity. The heat exchanger coating names in the legends correspond to the coatings listed in Table 3 and the test points along the x-axis correspond to the conditions listed in Table 6. The heat exchangers did not produce condensate at Test Point 4, so it's not included. Test Point 3 was not tested for all heat exchangers as the moisture condensate removal rate was already very low and almost undetectable for the heat exchangers tested. Additionally, the second hydrophilic coating (V2) was not tested at all points because Spring weather conditions did not allow the laboratory to consistently attain the cool, low humidity operating conditions. However, it is important to note that the second hydrophilic coating was outside of the scope of the original project.

Due to the number of heat exchangers and operating conditions tested and variation in performance across operating conditions, it is challenging to directly compare heat exchanger performance using Figure 28 and Figure 29. Figure 30 compares the uncoated and commercial radiator coating heat exchangers by first taking the mean from the two samples for a given operating condition. The orange line in Figure 30 is a linear regression comparing the commercial coating to the uncoated heat exchanger. The plot shows the commercial radiator coating hinders the moisture removal rate since the slope of the orange line is less than one, which is denoted by the gray, $y=x$ line.

Figure 31 shows the two conductive e-coating heat exchanger samples had similar performance and Figure 32 concludes the conductive e-coating performed similarly to the commercial radiator coating.

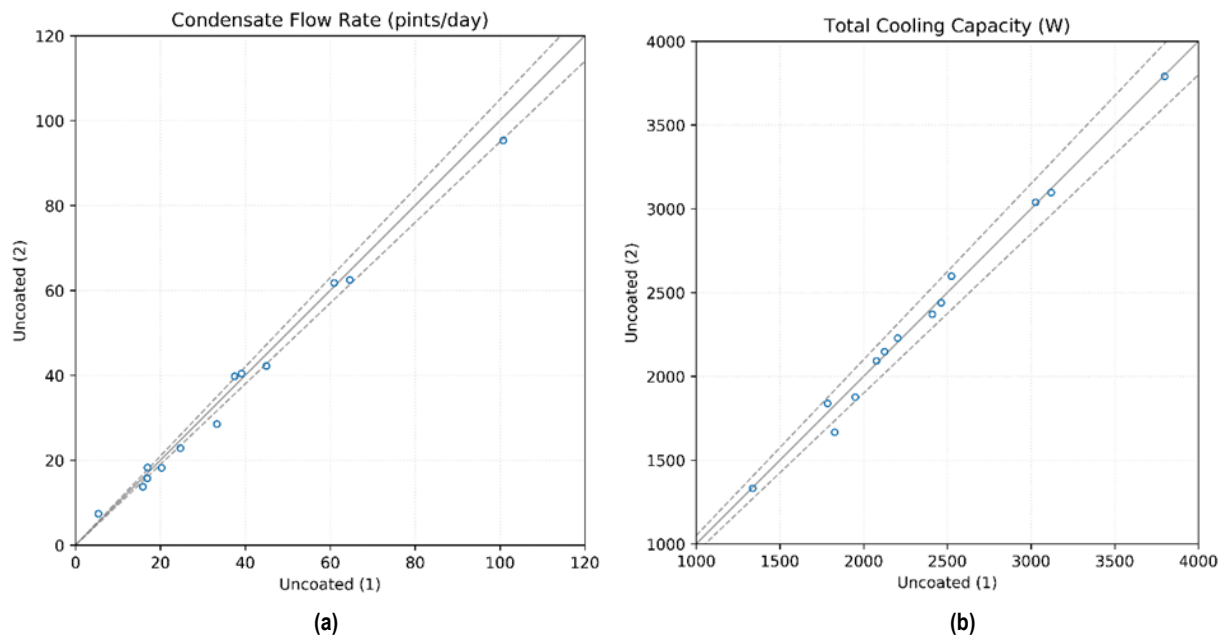


Figure 26. Scatter Plot Comparing (a) Moisture Removal Rate and (b) Total Cooling Capacity for Two Uncoated Heat Exchangers

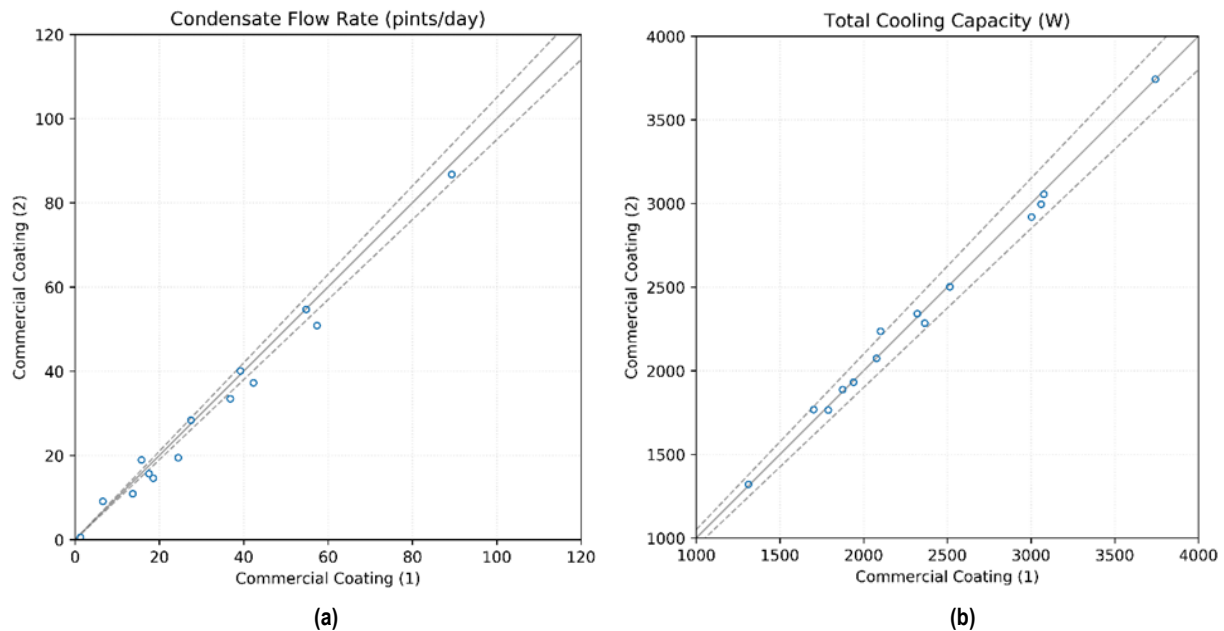


Figure 27. Scatter Plot Comparing (a) Moisture Removal Rate and (b) Total Cooling Capacity for Two Heat Exchangers with Commercial Radiator Coating

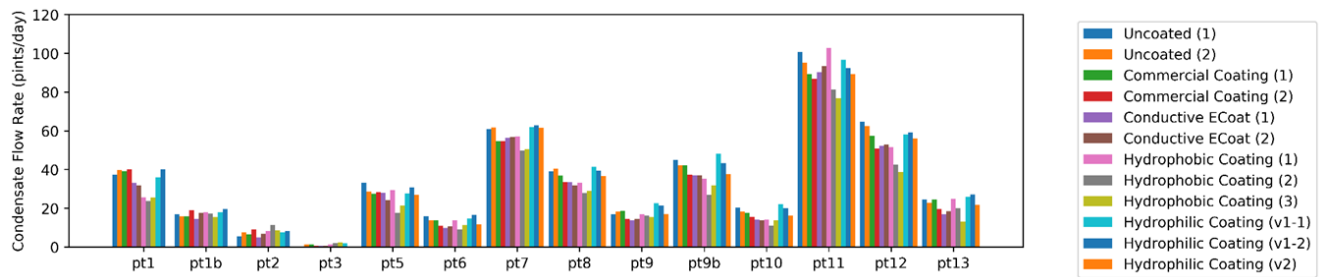


Figure 28. Average Moisture Removal Rate for All Heat Exchangers Tested at Various Conditions

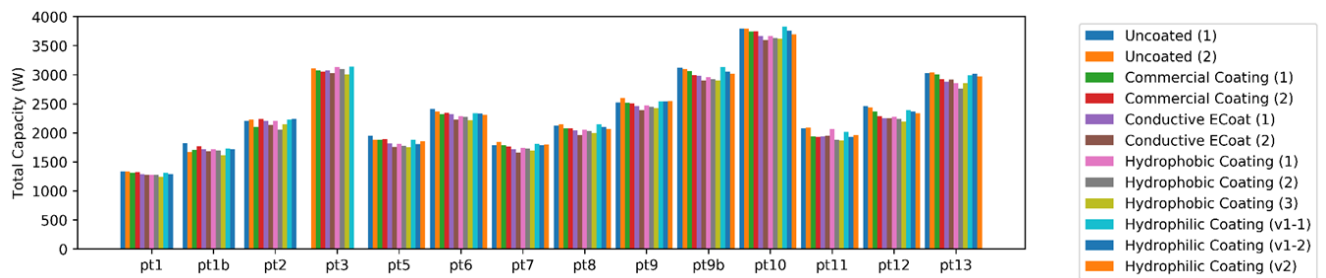


Figure 29. Total Cooling Capacity for All Heat Exchangers Tested at Various Conditions

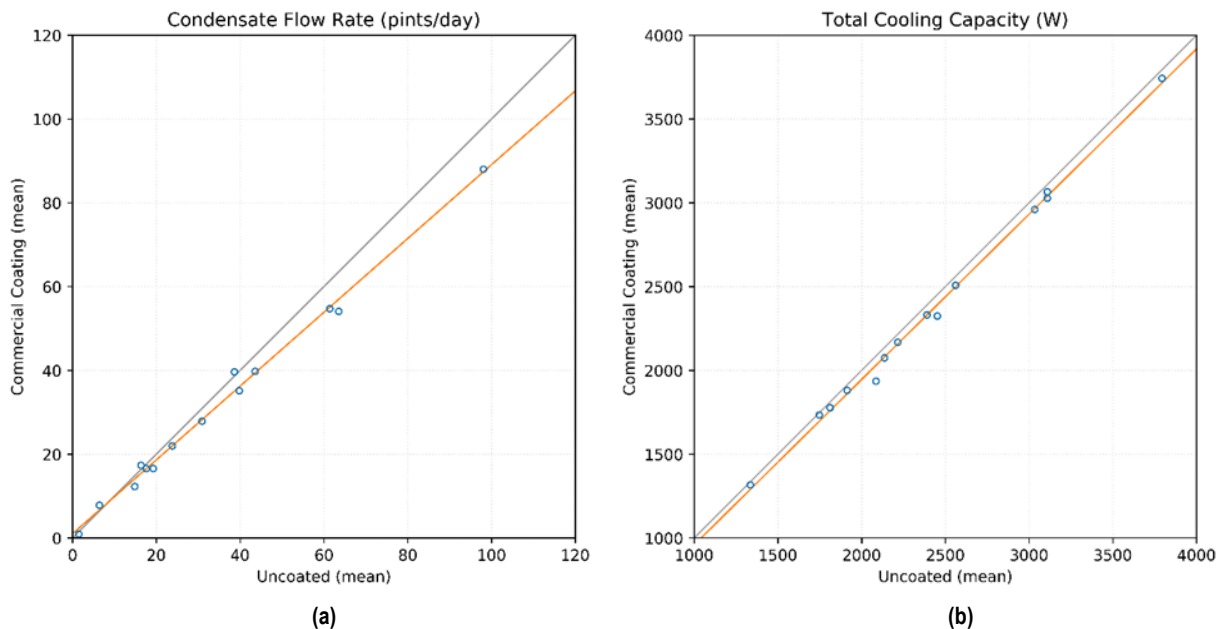


Figure 30. Scatter Plot Comparing (a) Moisture Removal Rate and (b) Total Cooling Capacity for Uncoated and Commercial Radiator Coating Heat Exchangers

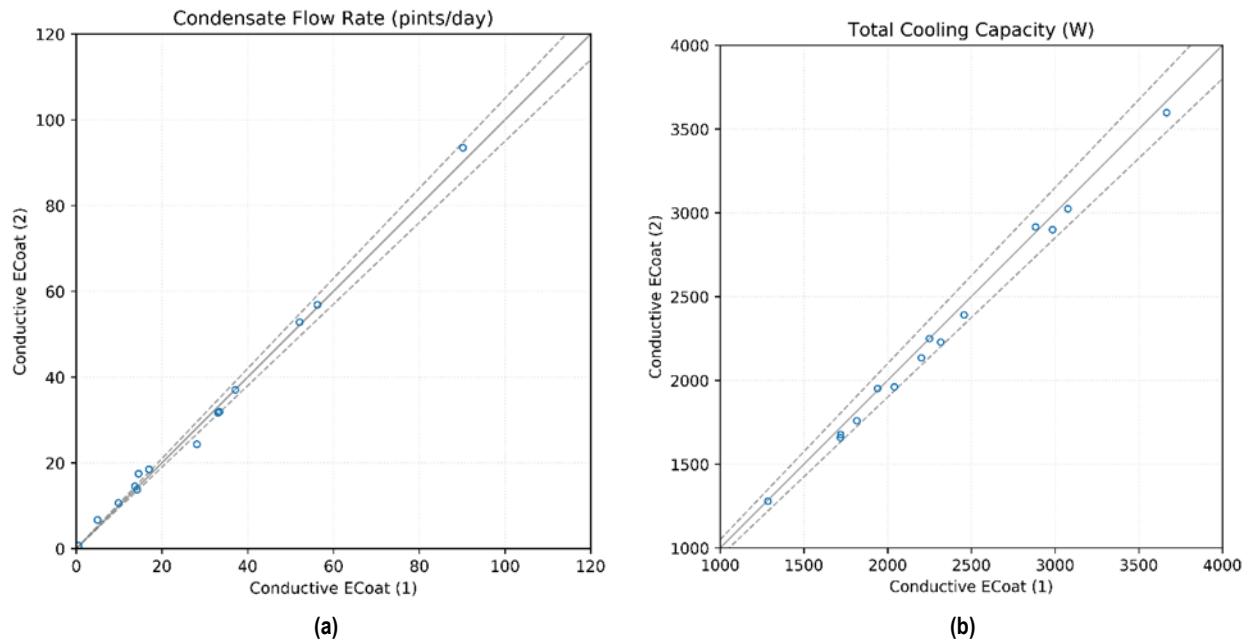


Figure 31. Scatter Plot Comparing (a) Moisture Removal Rate and (b) Total Cooling Capacity for Two Heat Exchangers with Conductive e-Coating

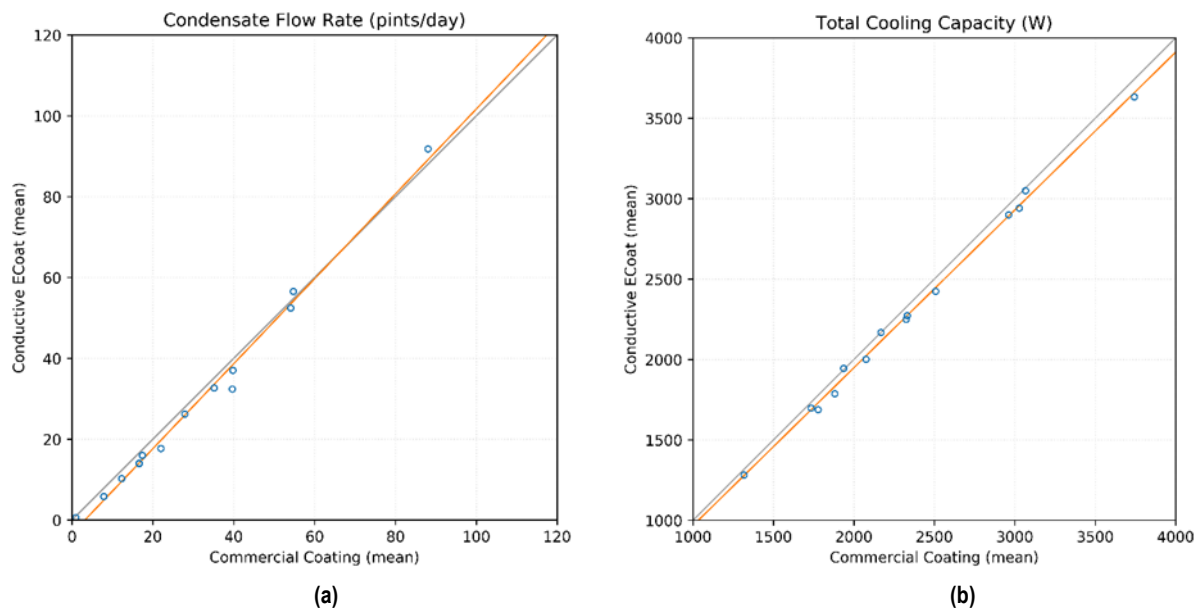


Figure 32. Scatter Plot Comparing (a) Moisture Removal Rate and (b) Total Cooling Capacity for Commercial Radiator and Conductive Coating Heat Exchangers

Figure 33a shows the variation between the first two hydrophobic heat exchanger samples was larger than the other coating types. Due to this variation, a third hydrophobic coated heat exchanger was tested, which performed similarly to the second sample as shown in Figure 34. Since the performance of the three hydrophobic coated heat exchangers varied

more than the other exchangers, comparisons to the heat exchangers with the commercial radiator coating are not plotted on an x-y scatter plot. However, hydrophobic coated heat exchanger performance can be compared to the other coatings by analyzing the bar plots in Figure 28 and Figure 29.

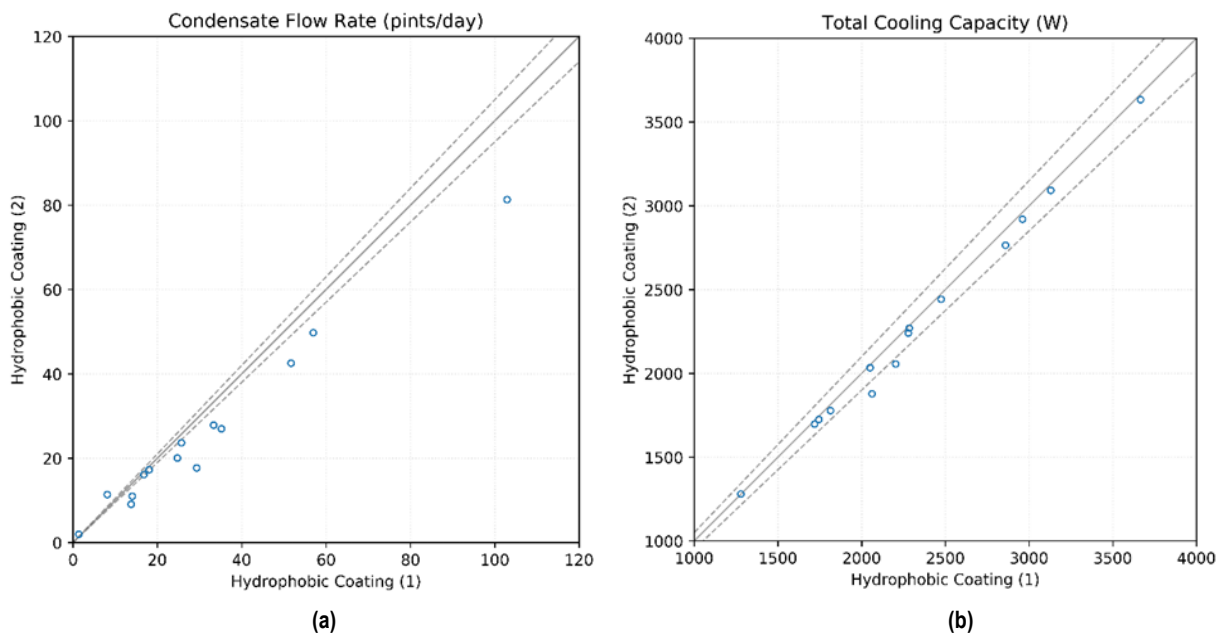


Figure 33. Scatter Plot Comparing (a) Moisture Removal Rate and (b) Total Cooling Capacity for Hydrophobic Coated Heat Exchanger Samples One and Two

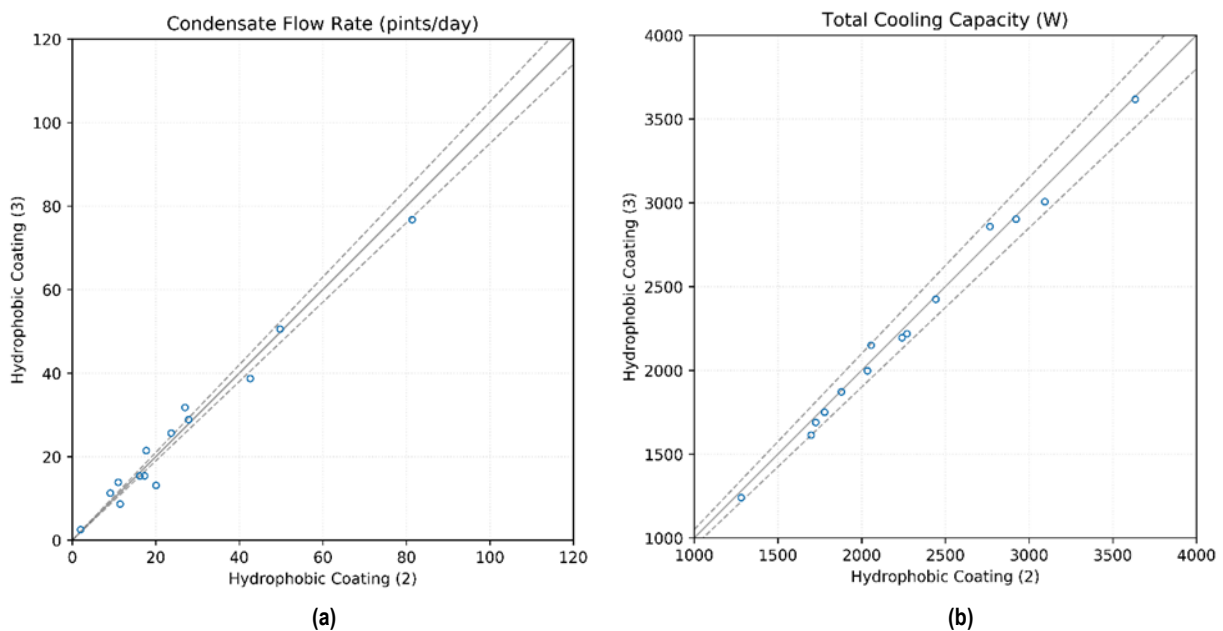


Figure 34. Scatter Plot Comparing (a) Moisture Removal Rate and (b) Total Cooling Capacity for Hydrophobic Coated Heat Exchanger Samples Two and Three

Figure 35 shows that the two hydrophilic coated heat exchangers had similar performance to one another. Figure 36 shows the hydrophilic coated heat exchangers had higher moisture removal rates than the commercial radiator coating. Due to this trend, a third hydrophilic coated heat

exchanger was tested at a limited number of operating conditions. From Figure 28, the third hydrophilic coated heat exchanger performed similarly to the first two hydrophilic coated heat exchangers.

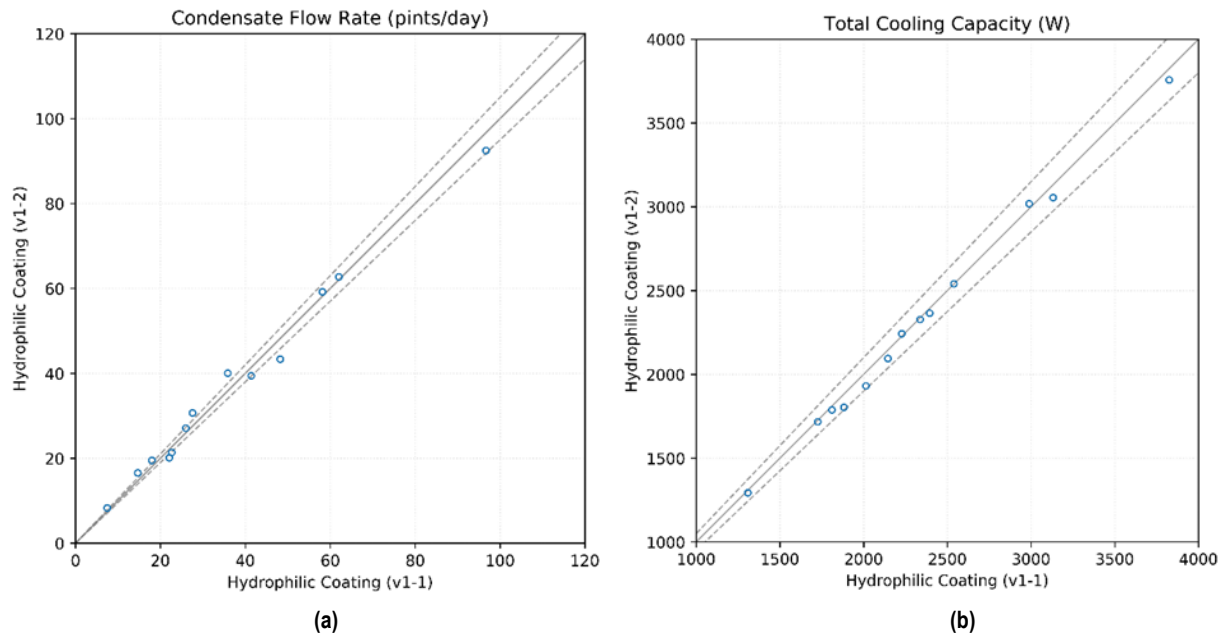


Figure 35. Scatter Plot Comparing (a) Moisture Removal Rate and (b) Total Cooling Capacity for Hydrophilic Coated Heat Exchanger Samples

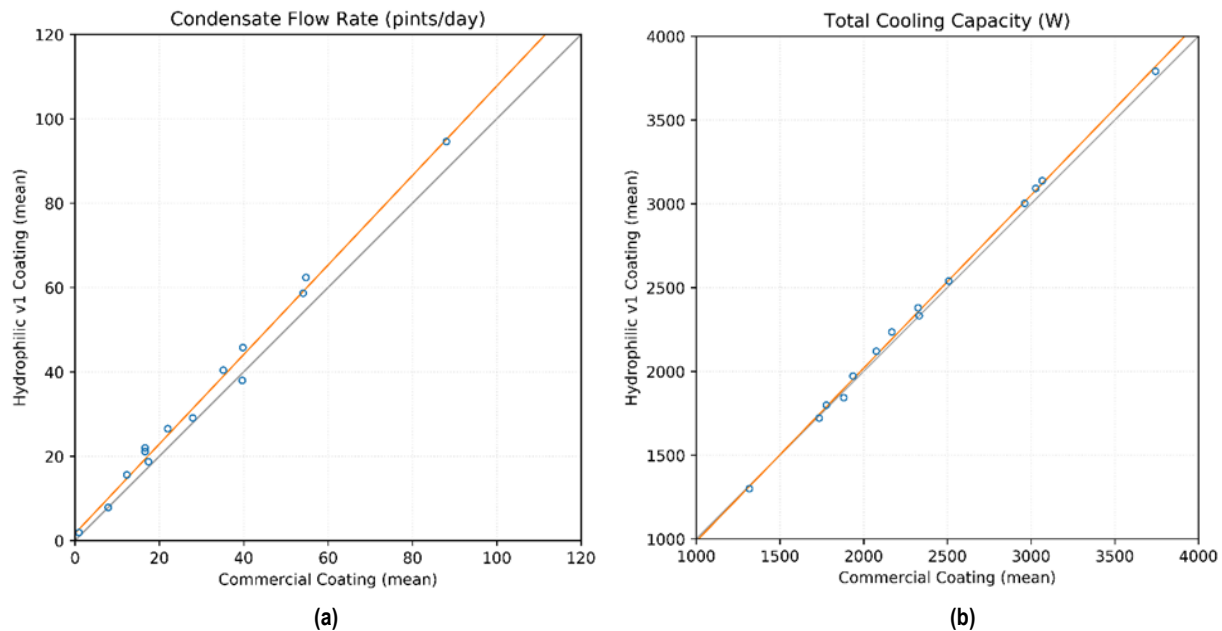


Figure 36. Scatter Plot Comparing (a) Moisture Removal Rate and (b) Total Cooling Capacity for Commercial Radiator and Hydrophilic Coated Heat Exchangers

4. Conclusions

The addition of various coatings (e.g. hydrophobic, hydrophilic, conductive, etc.) to a heat exchanger surface can be a quick and effective way to significantly influence the heat exchanger performance. Specifically, the addition of coatings can potentially improve the heat transfer effectiveness and moisture removal properties of a heat exchanger. PPG successfully prepared a wide range of coatings engineered to have surface energies ranging from hydrophilic to super-hydrophobic. The coatings included solvent- and water-based thermosets which could be applied to heat exchanger surfaces via dip, spray or electro-deposition techniques. While not all coatings would be suitable for application to the complex geometries of a fin and tube heat exchanger, they were all useful to test theories about water condensation on the heat exchanger surfaces. Particular effort was made to utilize electro-deposition coatings as these are already used in HVAC applications to protect equipment from corrosion in harsh environments. An electro-deposition coating which provided both corrosion resistance and improvements in heat exchanger efficiency would be of significant value to both commercial HVAC systems as well as water from air applications. Initial efforts to characterize performance of these coatings through a collaboration with UIUC researchers provided mixed results. While the UIUC team has excellent resources to characterize droplet formation and release properties, the surface area of the coated test articles was too small to detect water collection efficiency.

More information was obtained through a subsequent collaboration with the NREL. NREL was able to experimentally determine the role of four coatings that were developed by PPG that seek to improve heat exchanger performance. The experiments involved applying the different coatings to a series of heat exchangers with identical design and installing them in a custom-built heat exchanger plenum that interfaces with

the Advanced HVAC Laboratory at NREL's TTF. Cold glycol was supplied to the heat exchangers using a secondary loop thermally connected with a 20-ton capacity chiller loop, which conditioned the glycol to the desired temperature. The primary performance metrics used to evaluate the heat exchanger performance were moisture removal rate, measured by collecting and weighing condensate, and the total heat transfer rate. The performance metrics were determined for various operating conditions and compared for each heat exchanger sample.

Two heat exchangers for each coating type were tested to assess variability in heat exchanger performance and consistency with the coating process. NREL results showed high agreement between the measured values for most of the heat exchanger coatings (meaning, results were approximately within $\pm 5\%$ for identical heat exchanger coatings applied to different test heat exchangers). The variation between the two first hydrophobic coated heat exchangers was greater than the previously tested heat exchangers, so a third hydrophobic coated heat exchanger was evaluated.

When comparing the influence of different heat exchanger coatings, NREL found the commercial coating hindered moisture removal compared to the uncoated heat exchangers. This was entirely expected as the commercial coatings were designed for corrosion protection and not heat exchanger efficiency. Increased heat transfer resistance from the organic coating thickness may also be a contributor to decreased efficiency. The hydrophilic coated heat exchangers typically had the highest moisture removal rates. Although the hydrophilic coated heat exchanger showed an increase in the moisture removal rate, the cooling capacity did not show as drastic of an increase. The hydrophilic coating was also much lower than the electrodeposition coatings in total film thickness, accordingly less heat transfer resistance might be expected. Figure 37

provides a summary of the average increase or decrease in water collection rates across all test conditions. Using the uncoated heat exchanger as a control a net increase of 8% is observed for the hydrophilic coating whereas hydrophobic electrodeposition coatings reduced water collection relative to the control. This is a significant finding that warrants further investigation.

Although the results typically showed the hydrophilic coating had a higher moisture removal rate than the hydrophobic coating, which may seem counter-intuitive, it was

concluded that this discrepancy may be influenced by the heat exchanger design, such as fin and tube density. It is recommended that future studies consider using heat exchangers of different design to further investigate the effects of these coatings on heat exchanger performance. Further, additional work should be done in developing hydrophilic coatings, particularly hydrophilic electrodeposition coatings which would potentially provide all of the desired features of corrosion protection, uniform application to complex heat exchanger geometries and increased efficiency of water removal.

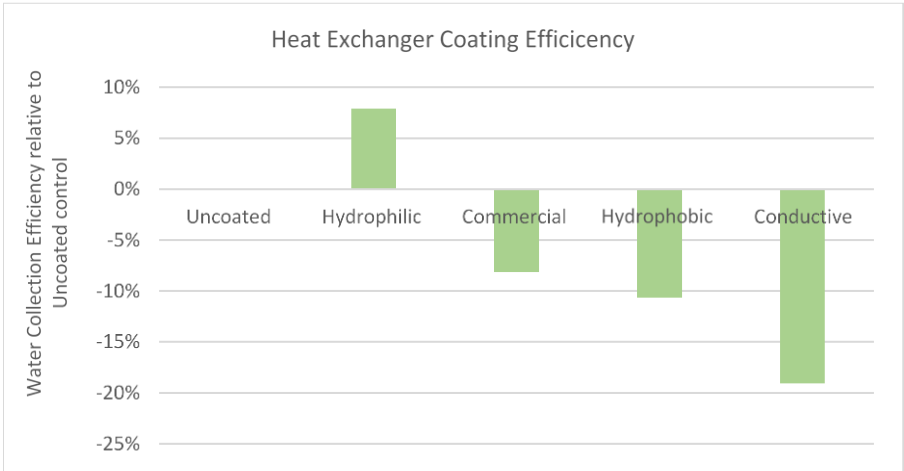


Figure 37. Comparison of Water Collection Rates for Coated Heat Exchangers Relative to Uncoated Control

5. Recommendations

The project data presented in this report provides some surprising insights into feasibility of developing coatings which can enhance water harvesting from air. However, a fieldable solution would require coatings with long-term durability that also retain the hydrophilic nature over the life of the AC unit to become a commercially viable technology. In addition, this project made no effort to examine unintended effects of hydrophilic coatings on the heat exchanger components such as corrosion of fin and tube assemblies, quality of water collected, effect on defrost cycles or expenses related to adding an additional manufacturing step in the HVAC system fabrication.

So while hydrophilic coatings represent an opportunity to support the warfighter, the consumer and the environment, additional work is required to develop, test and optimize coatings which could realistically become a standard practice within the industry. Electrodeposition coatings are particularly well suited to the application by virtue of their ability to form uniform thin films over complex geometries, their extremely high transfer efficiency and low environmental impact but these coatings are typically hydrophobic. Inventions are required to create hydrophilic electrodeposition coatings which retain their other desirable features.

6. References

- [1] Water Support Operations, ATP 4-44/MCRP 3-17.7Q, October 2015.
- [2] Bain, R., Johnston, R., Mitis, F., Chatterley, C. and Slaymaker, T. Establishing Sustainable Development Goal Baselines for Household Drinking Water, Sanitation and Hygiene Services. *Water*, 10, 1711, 2018.
- [3] Progress on Drinking Water, Sanitation and Hygiene: 2017 Update and SDG Baselines. World Health Organization and the United Nations Children's Fund, 2017.
- [4] Global Indicator Framework for the Sustainable Development Goals and Targets of the 2030 Agenda for Sustainable Development. United Nations, 2018.
- [5] <https://rainmakerww.com/technology-air-to-water/>
- [6] <https://seas-sa.com/project/water-wells-from-sky-with-photovoltaic-energy/>
- [7] <https://news.climate.columbia.edu/2011/03/07/the-fog-collectors-harvesting-water-from-thin-air/>
- [8] Enright, R, Miljkovic, N, Alvarado, JL, Kim, K, and Rose, JW. Dropwise Condensation on Micro- and Nanostructured Surfaces. United States: N. p., 2014. Web. doi:10.1080/15567265.2013.862889.
- [9] Ramachandran, R. and Zosonovsky, M. Vibrations and Spatial Patterns Change Effective Wetting Properties of Superhydrophobic and Regular Membranes. United States. Biomimetics, August 2016.
- [10] Nenad, Miljkovic et al. Condensation on Hydrophilic, Hydrophobic, Nanostructured Superhydrophobic and Oil-Infused Surfaces. *Journal of Heat Transfer*, 135.8 (2013): 080906.
- [11] X. Ma et al. Effects of Hydrophilic Coating on Air Side Heat Transfer and Friction Characteristics of Wavy Fin and Tube Heat Exchangers Under Dehumidifying Conditions. *Energy Conversion and Management*, 48, 2525-2532, 2007.
- [12] <https://gentoocoating.com/test-data-hydrophobicity-transparency/>
- [13] Winkler, J., Christensen, D., and Tomerlin, J. Laboratory Test Report for Six ENERGY STAR Dehumidifiers. United States: N. p., 2011. Web. doi:10.2172/1032386.
- [14] Yin, P. and Sang, Y. Model-Based Sensitivity Analysis of Barometric Pressure on Cooling Capacity Measurement of Hydronic Room Fan Coil Units. *Science and Technology for the Built Environment*, 27(3), 316-328, 2020.
- [15] ASHRAE, 2016. ANSI/ASHRAE Standard 33-2016: Methods of Testing Forced-Circulation Air-Cooling and Air-Heating Coils.
- [16] [Decarbonizing U.S. Buildings | Center for Climate and Energy Solutions \(c2es.org\)](https://www.c2es.org/decarbonizing-us-buildings/)